

Chromosomal Instability in Aneuploid Cells

Master Thesis in Biology

at the Max Planck Institute of Biochemistry

in the Group of Dr. Zuzana Storchova

(Department Molecular Cell Biology)

by

Giuliana Katharina Lott

Duration of the thesis: 31.03.2014-29.09.2014

Declaration

I hereby confirm that I have written the accompanying thesis by myself, without contributions from any sources other than those cited in the text and acknowledgments. This applies also to all graphics, drawings, maps and images included in the thesis.

Munich,

Gutachter: Herr Professor Dr. Stefan Jentsch

Table of Contents

1	Zusammenfassung	4
2	Abstract	6
3	Introduction	8
3.1	Tetraploidy, aneuploidy and chromosomal instability	8
3.2	Mechanisms that may cause chromosomal instability	10
3.3	Post-tetraploids as a model system for complex aneuploidy	11
3.4	Tolerance to chromosome missegregation	12
4	Results	17
4.1	Characterization of RPE1 derived post-tetraploids (RPTs)	17
4.2	Accumulation of nuclear p53 upon missegregation in PTs	21
4.3	Changes in the abundance of p53 in post-tetraploids after induced missegregation	23
4.4	Changes in the abundance of p53 and p38 in post-tetraploids upon induced DNA damage	25
5	Discussion	28
5.1	Post-tetraploids derived from a non-transformed cell line are aneuploid and chromosomally unstable	28
5.2	Nuclear p53 enrichment is attenuated after micronucleation in post-tetraploid cells	30
5.3	Mechanisms that can contribute to tolerance to mitotic errors in PTs	31
5.4	Response to DNA damage is altered in PTs	33
5.5	Oxidative DNA damage could be sensed less efficiently in PTs	34
6	Materials and Methods	37
6.1	Cell lines	37
6.2	Primary antibodies	38
6.3	Materials and solutions	38
6.3.1	SDS-PAGE and immunoblotting materials	38
6.3.2	Other materials	39
6.4	Cell culture	39
6.4.1	Working cell stocks	39
6.4.2	Culturing	39

6.5	Mycotrace	40
6.6	Used drugs to assess p53 response	40
6.7	Cell lysis, protein preparation and concentration measurement	41
6.8	SDS-PAGE and immunoblotting	41
6.9	Micronucleation test	42
6.10	Analysis of mitotic abnormalities	42
6.11	Interphase FISH	42
6.12	Copy Number Analysis	43
7	Supplementaries	45
8	Literature	47
9	Acknowledgments	59

List of Figures

1	Tetraploidy as an intermediate route to aneuploidy and CIN.	9
2	Generation and characterization of post-tetraploid (PT) cell lines	13
3	Survival after mitotic errors	14
4	Characterization of post-tetraploid cell lines derived from RPE1	18
5	Copy number analysis of HCT116, HPT1, RPE1 and RPT3 by SNParray data .	19
6	Post-tetraploids deregulate the p53 signaling pathway	22
7	Activation of p53 after Vs83-induced missegregation	24
8	Post-tetraploids deregulate the p53 signaling pathway upon induced DNA damage	26
S1	Test for mycoplasm infection in all cell lines	45
S2	Characterization of post-tetraploid cell lines derived from RPE1 and HCT116 .	45
S3	Mitotic spindle is altered in HPTs	46
S4	Changes in microtubule polymerization in HPTs	46

List of Tables

1	Used cell lines and descriptions	37
2	Primary antibodies	38
3	Mycotrace	40

1 Zusammenfassung

Tetraploidie, ein Zustand, in dem Zellen vier haploide Chromosomensätze aufweisen, kann ein Weg zu Aneuploidie, welche durch Abweichungen in Anzahl und Struktur der Chromosomen gekennzeichnet ist, sein. Aneuploidie ist oft ein Ausdruck von im Gleichgewicht von Chromosomverlust und -gewinn befindlicher chromosomaler Instabilität (Chromosomal Instability, kurz CIN). Chromosomale Instabilität ist durch Chromosomen-Misssegregation gekennzeichnet und wird zusammen mit Aneuploidie oft in Tumoren beobachtet. CIN ermöglicht es Tumoren, sich an ihre Umweltbedingungen anzupassen und wird deshalb mit Arzneimittelresistenz und schlechten Prognosen bei Krebserkrankungen verbunden. Alles in allem legt dies eine Route von transient auftretender Tetraploidität zu Tumorentstehung nahe.

Aus diesem Grund wurde in unserem Labor ein Modell der Evolution tetraploider Zellen entwickelt, indem die Zytokinese in sowohl krebsartigen (HCT116) als auch nicht krebsartigen, immortalisierten Zellen (RPE1 hTERT) inhibiert wurde. Die Nachkommen, welche diese Tetraploidisierung überlebt hatten, sogenannte post-Tetraploide (PT), wurden nach ihren parentalen Zelllinien HPTs und RPTs genannt. HPTs weisen Aneuploidie und CIN auf, welches sich unter anderem in erhöhten Raten mitotischer Fehler wie nachhängenden Chromosomen und Anaphasenbrücken, zeigt. Außerdem sind HPTs toleranter gegenüber Misseggregation, was sich darin äußert, dass sie bipolare mitotische Misseggregationen häufiger überleben.

Um herauszufinden, ob PTs, welche von einer immortalisierten Zelllinie abstammen, einen Misseggregations-Phänotyp sowie Aneuploidie und CIN aufweisen, habe ich Fluoreszenz *In Situ* Hybridisierungs-Experimente (FISH) an centromerischen Regionen der Chromosomen 3 und 7 durchgeführt. Des Weiteren wurde die Anzahl an Kopien jedes Chromosoms bestimmt. RPT3, die einzige RPE1 hTERT-Nachkommenlinie, welche erhöhte Misseggregationsraten aufweist, zeigte ebenfalls Aneuploidie.

Da der Arrest neu gebildeter tetraploider Zellen von p53 abhängt, könnte eine Deregulierung von Mitgliedern des p53-Signalwegs zu Toleranz gegenüber Misseggregation führen. Dies wurde schon für HPTs mittels einer Mikronukleation-Analyse gezeigt. Hierbei wurde das nukleare p53-Signal in binuklearen Zellen, welche Mikronuklei enthielten, getestet. Mikronukleation ist einer der Phänotypen, die durch Misseggregation entstehen können. PTs, welche ihre Chromosomen häufiger als ihre parentalen Zelllinien missegregieren, haben ein vermindertes p53-Signal im Nukleus.

Dies führte zur Untersuchung, ob die reduzierte Aktivierung von p53 mit Misseggregation korreliert. Hierzu wurde Misseggregation induziert gefolgt von Immunoblotting-Experimenten gegen

p53 und pSer15-p53. Es wurde jedoch keine Verbindung zwischen induzierter Misssegregation und verminderter p53-Aktivierung gefunden.

Folglich untersuchte ich, ob eine andere Art zellulären Stresses den p53-Signalweg stören würde. DNA-Schäden sind eine Art zellulären Stresses, auf den p53 reagiert. Ich führte Immunoblotting-Experimente an unbehandelten Proben sowie an Proben, die mit DRB, einer DNA-schädigenden Substanz, behandelt wurden, durch. Die Aktivierung von p53 war in DRB-behandelten Zellen gestört. Um herauszufinden, ob dies durch p53 selbst, durch einen Aktivator von p53 oder beides verursacht wird, untersuchte ich, ob die Upstream-Aktivierung von p53 ebenfalls gestört ist. p38 war ein guter Kandidat, da es p53 an Serin 15 phosphoryliert und mit p53-Aktivierung bei chromosomaler Misssegregation in Verbindung gebracht worden ist. Sowohl p38 als auch p53 scheinen eine verminderte Aktivierung in DNA-schädigenden Bedingungen aufzuweisen.

2 Abstract

Tetraploidy, a cellular state where cells harbor four haploid sets of chromosomes, can be a route to aneuploidy, which is defined by alterations in chromosome number and structure. Aneuploidy itself is often a steady-state manifestation of chromosomal instability (CIN). Chromosome missegregation is a hallmark of CIN. Aneuploidy and CIN are often observed in tumors. CIN enables tumors to adapt to their environment and is therefore associated with drug resistance and poor prognosis in cancer. Taken together, a route from transient tetraploidy to aneuploidy and CIN to tumorigenesis was proposed.

Therefore, in our lab, a model mimicking the evolution of tetraploid cells was generated by inhibiting cytokinesis in both cancerous (HCT116) and non-cancerous, immortalized (RPE1 hTERT) cell lines. According to their parental cell lines, the resulting progeny that survived tetraploidization, so-called post-tetraploids (PTs), were called HPTs and RPTs, respectively. HPTs display aneuploidy and CIN, manifested in increased rates of mitotic errors, e.g. lagging chromosomes and anaphase bridges. Furthermore, HPTs are more tolerant to missegregation in a way that they display increased survival in response to chromosome missegregation in bipolar mitosis.

To investigate whether PTs derived from an immortalized cell line displayed the missegregation phenotype, aneuploidy and CIN, I performed Fluorescence *In Situ* Hybridization (FISH) experiments on centromeric regions of chromosome 3 and 7. Additionally, the chromosome copy numbers were analyzed. RPT3, the only RPE1 hTERT derived cell line that displayed increased rates of missegregation, displayed complex aneuploidy, as well.

Since freshly arising tetraploids arrest in a p53-dependent manner, a deregulation of members of the p53 pathway could lead to tolerance to missegregation. This was already shown for HPTs in a micronucleation analysis. In this analysis, the nuclear p53 signal in binucleated cells containing micronuclei was assessed. Micronucleation is one phenotype of missegregation. PTs, which missegregate their chromosomes more often than their parental cell lines showed a decreased nuclear p53 signal after micronucleation.

This fact led me to investigate whether the decreased p53 activation correlates to missegregation. The approach chosen was inducing missegregation followed by immunoblotting experiments against p53 and pSer15-p53. This, however, did not yield any link between induced missegregation and decreased p53 activation.

Therefore I investigated if a different kind of cellular stress would result in an impaired p53 pathway. One of the cellular stresses sensed by p53 is DNA damage. I performed immunoblot-

ting experiments in untreated samples and samples treated with a DNA damaging reagent, DRB. The activation of p53 was changed in DRB-treated samples. To address the question whether this is caused by p53 itself or by an activator of p53 or both, I investigated if the upstream activation was also impaired. p38 was a good candidate since it phosphorylates p53 on serine 15 directly and is associated with p53 activation upon chromosome missegregation. Both p38 and p53 seem to show decreased activation in DNA-damaging conditions.

3 Introduction

3.1 Tetraploidy, aneuploidy and chromosomal instability

Tetraploidy is a cellular state in which cells harbor four haploid sets of chromosomes. It can arise via three main mechanisms: cell fusion, mitotic slippage or failure of cytokinesis (for review: Storchova and Pellman (2004)).

Cell fusion is frequently a part of developmental processes, such as muscle development in *D. melanogaster*. In this process, muscle progenitor cells fuse with undifferentiated, neighboring muscle founder cells to form myoblasts (Ruiz Gómez and Bate, 1997; Landgraf et al., 1999). In addition, cells fuse as a consequence of virus infections e.g. human herpes virus 7 infections, which can lead to CD4-positive T-cell fusion (Secchiero et al., 1998). Furthermore, Sendai virus causes human cells to fuse in culture (Migeon et al., 1974). Finally, viral infection can trigger cell fusion which results in CIN and cancer. The otherwise unharful virus MPMV induces massive instability in fused cells, which express the oncogenes E1A and HRAS. This prevents the cells from dying after the E1A transduction after cell fusion. When these cells were injected into mice, these mice developed tumors, whereas mice injected with control cells with co-transduced oncogenes and control cells, which were injected with MPMV virus and co-transduced with the oncogenes but were never fused, did not develop any tumors (Duell et al., 2007).

Mitotic slippage is a process caused by premature transition from mitosis to G1 phase. This phenomenon is normally hindered by the spindle assembly checkpoint (SAC), which controls proper microtubule-kinetochore attachments. Weakly attached kinetochores normally activate the SAC, which prevents the anaphase-promoting complex (APC) from degrading cyclin B (Brito and Rieder, 2006) (for review: Musacchio and Salmon (2007)). Mitotic slippage is a consequence of premature cyclin B degradation by the proteasome that drives cells out of mitosis. This slippage can take place even despite existing mitotic defects.

The third mechanism leading to tetraploidy is a cytokinesis failure that results in formation of binucleated cells. Cytokinesis failure takes place when nuclear DNA is trapped between the daughter cells or even if one chromosome lags between them (Mullins and Bieseile, 1977; Shi and King, 2005). Cytokinesis failure can be caused by the impairment of spindle elongation (Margall-Ducos et al., 2007), telomeric dysfunction leading to anaphase bridges (Pampalona et al., 2012) or through mutations in the tumor suppressor Adenomatous Polyposis Coli (APC) (Caldwell et al., 2007) (for review Normand and King (2010)). Experimentally, cytokinesis fail-

ure can be induced by treatment of cells with the drug dihydrocytochalasin and its derivatives that prevent the remodeling of the actin cytoskeleton and cleavage furrow progression during cytokinesis (Fujiwara et al., 2005; Kuffer et al., 2013).

Tetraploid cells arise in mammalian organs and tissues as a part of the developmental program or as a cellular reaction to metabolic stress (Guidotti et al., 2003). On the other hand, unscheduled tetraploidization can have detrimental effects, such as cell transformations (Fujiwara et al., 2005) and miscarriages (Eiben et al., 1990; Hassold and Chiu, 1985) (for review: Storchova and Kuffer (2008)). Recently it has been suggested that tetraploidy could be a route to aneuploidy, a cellular state characterized by abnormal karyotypes and multiple structural and numerical chromosomal aberrations. Furthermore, aneuploidy is frequently a steady-state manifestation of chromosomal instability (CIN) – a persistent dynamic state, characterized by continuous chromosome losses and gains (for review see: Storchova and Kuffer (2008); Gordon et al. (2012); Fig. 1).

In 1902, Theodore Boveri proposed that tetraploidization, achieved in his case by double fertilization of sea urchin eggs, leads to multipolar mitosis. Multipolar mitosis causes chromosome missegregation, which in turn results in abnormal chromosome numbers in daughter cells. These abnormal chromosome numbers - aneuploidy - might cause tumorigenesis (Boveri, 2008). Multipolar mitosis occurs due to abnormal centrosomal numbers (for review: Nigg (2002)). Indeed, it was observed that upon p53 inactivation in Barrett's esophagus, tetraploid cells give rise to aneuploids (Galipeau et al., 1996). Furthermore, a direct link between tetraploidy and tumorigenesis was shown by Fujiwara (Fujiwara et al., 2005). They injected diploid and tetraploid cells into mice and observed that only a subset of mice injected with tetraploid cells formed tumors, whereas none of the mice injected with diploid cell formed tumors. The observed tumors showed near-tetraploid karyotypes with chromosome gains and losses as well as structural chromosomal rearrangements.

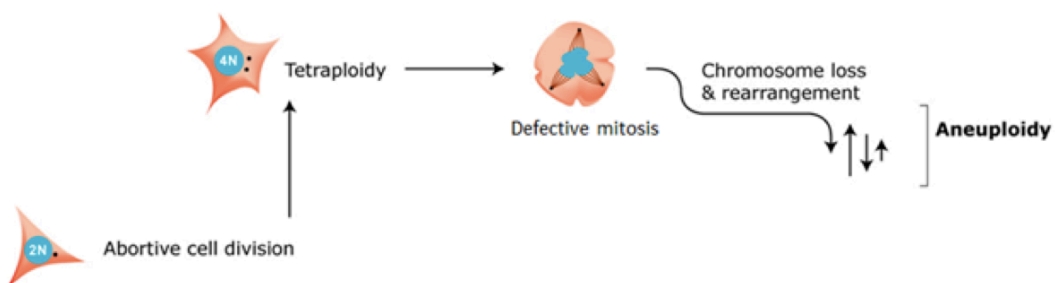


Fig. 1: **Tetraploidy as an intermediate route to aneuploidy and CIN.** Figure from Kuznetsova (2013).

Aneuploidy itself is observed in most malignant tumors (for review: Storchova and Kuffer (2008); Gordon et al. (2012)). Somatic copy number alterations are very common in cancer samples and cannot be explained by known cancer target genes (Beroukhim et al., 2010). It was proposed that high levels of aneuploidy are a steady-state manifestation of CIN (Thompson and Compton, 2010).

CIN is defined by ongoing chromosome number changes and chromosomal rearrangements. It was proposed that increased mutation rates due to CIN could lead to unbalanced expression of regulatory and structural genes (Duesberg et al., 2000). Therefore it is not surprising that CIN can lead to tumor formation in mice (Wang et al., 2006). and is associated with solid tumors such as colorectal and lung cancer (Haruki et al., 2001; Lengauer et al., 1997). Furthermore, tetraploidy and CIN were observed as early events in cervical cancer (Olaharski et al., 2006). CIN is associated with drug resistance and poor prognosis (Duesberg et al., 2000; Carter et al., 2006). It enables tumors to adapt to changes in their environment better than normal diploid cells (Bakhoun and Compton, 2012). Cancer arises over years which is why a heterogeneous cell population could evolve from a single, genetically unstable cell which has overcome proliferation barriers and evaded defenses against uncontrolled proliferation (Anderson et al., 2001). To sum up, tetraploidy may be an intermediate route to aneuploidy and CIN. The latter causes heterogeneity in tissues which contributes to chromosome changes in cancer. Changes in chromosome structure lead to the loss of tumor suppressor loci and copy number gains in oncogenes, which could result in cancer.

3.2 Mechanisms that may cause chromosomal instability

As already stated, aneuploidy is often a steady-state manifestation of CIN (for review see: Storchova and Kuffer (2008); Gordon et al. (2012)). Aneuploid genomes have a higher susceptibility to chromosome damage, which is often observed in tumor cells (Matzke et al., 2003). It was hypothesized that aneuploidy may lead to protein imbalances because of changes in chromosome numbers. These imbalances may cause insufficient control in chromosome segregation and may lead to defective mitosis. This could cause more and more severe aneuploid phenotypes and result in CIN (Duesberg and Li, 2003).

The occurrence of multiple centrosomes was established as a cause for CIN (Boveri, 2008; Nigg, 2002). There are four main causes of multiple centrosomes: centrosome overduplication, abortive cell division, cell fusion and *de novo* formation of centrosomes (for review: Nigg (2002)). Multiple centrosomes can cause multipolar mitosis and cells undergoing multipolar

mitosis segregate their chromosomes in a near-random fashion (Gisselsson et al., 2008; Doxsey et al., 2005). Cells with an abnormal number of centrosomes can cluster centrosomes to form a bipolar spindle (Kwon et al., 2008). However, a study revealed that even clustered centrosomes cause missegregation, since they form a multipolar intermediate (Ganem et al., 2009).

A defective Spindle Assembly Checkpoint (SAC) can cause CIN, as well. The SAC machinery controls the proper attachments of the kinetochores by microtubules and hinders anaphase onset in case of unattached or weakly attached kinetochores (for review: Musacchio and Salmon (2007)). Merotely is a state in which microtubules from both cell poles attach to the same kinetochore of one single chromatid. Merotelic attachment leads to lagging chromosomes since they are under pulling force from both spindle poles and their kinetochore gets stretched in this event. Lagging chromosomes lead to chromosome loss during mitosis and are therefore a cause for CIN (Cimini et al., 2001). Furthermore, mutations in SAC genes, such as Mad2 or Bub1 cause CIN (Michel et al., 2001; Cahill et al., 1998).

Changes in microtubule dynamics are also an important factor, which can contribute to CIN. Microtubule dynamics are regulated by a huge number of microtubule associated proteins (MAPs). Destabilizing MAPs are katanin, spastin and fidgetin (Sharp and Ross, 2012). Mutations in spastin can cause cytokinesis failure (Connell et al., 2009). An example for a stabilizing MAP is TPX2. It is necessary for spindle formation and chromosome segregation (Aguirre-Portolés et al., 2012).

Taken together, there is a plethora of different mechanisms by which cells may become chromosomally unstable. It is however not known which of the above mentioned mechanisms contributes to CIN in human cancer.

3.3 Post-tetraploids as a model system for complex aneuploidy

A model mimicking the evolution of tetraploid cells was previously generated in our laboratory using HCT116 (human hereditary nonpolyposis colon cancer) and the non-transformed, immortalized cell line RPE1 hTERT (retinal pigment epithelium cells, immortalized by expression of telomerase). Both cell lines are p53-proficient. All cell lines express H2B-GFP that allows visualization by live cell fluorescent microscopy. Tetraploid cells were generated by induced cytokinesis failure by treatment with dihydrocytochalasin D (DCD) (Fujiwara et al., 2005). Following drug release, cells were subcloned by limited dilution on 96-well plates. The DNA content in the progeny was assessed using flow cytometry for individual clones (Fig. 2 A, B).

All isolated HCT116-derived clones were termed HPTs and all RPE1 hTERT derived were termed RPTs.

HPTs showed no significant differences in the length of interphase (nuclear envelope breakdown to anaphase onset, Fig. 2 C) and they proliferate at the same rate as their diploid counterparts (Fig. 2 D). Both HPTs and RPTs displayed strong variation in their number of chromosomes from near-diploid to near tetraploid, indicating a numerical aneuploidy with variable karyotypes. HPTs displayed ongoing changes in chromosome numbers indicating that they do not only have complex aneuploidy but also chromosomal instability (Fig. 2 E). Additionally, HPTs display a higher number in translocations compared to their parental cell line HCT116 (Kuznetsova, 2013).

3.4 Tolerance to chromosome missegregation

As tetraploidy can be a potentially harmful precursor state for aneuploidy and CIN, certain cellular mechanisms prevent newly arising tetraploid cells from proliferating further. Data from our laboratory show that upon induction of cytokinesis failure most tetraploid cells can enter several consecutive mitoses and afterwards arrest and/or subsequently die in a p53-dependent manner (Kuffer et al., 2013). Interestingly, around 1% of tetraploid progeny is able to proliferate further. Those rare survivors, further referred to as post-tetraploids (PTs), displayed variable alterations in chromosome number and structure (aneuploidy) with predominant chromosome losses, as well as chromosomal instability. CIN manifests itself in an increase in mitotic errors (Fig. 3 A, B) and increased survival in response to bipolar chromosome missegregation observed in HPTs (Fig. 3 D, Kuznetsova (2013)). Interestingly, the increased frequencies of mitotic errors in HPTs are not the result of an abnormal number of centromeres (Kuznetsova, 2013). Similar findings were reported for spontaneously arising tetraploid cells that become more tolerant to chromosome missegregation than their progenitor diploid cells (Dewhurst et al., 2014).

The fact that aneuploid derivatives of tetraploid cells are able to proliferate in a CIN state instead of arresting in a p53-dependent manner suggests that deregulation of the p53 pathway may at least partially contribute to tolerance to mitotic defects in post-tetraploid cells. Understanding the mechanisms that allow proliferation of tetraploid progeny following chromosome missegregation might improve our knowledge of the link between p53 deregulation and CIN that are both frequently found in cancer. p53, the human transcription factor encoded by TP53, is a tumor suppressor which functions mainly as a homo-tetramer. It consists of an amino-terminal transactivation domain, a DNA-binding domain (DBD) and a carboxy-terminal tetrameriza-

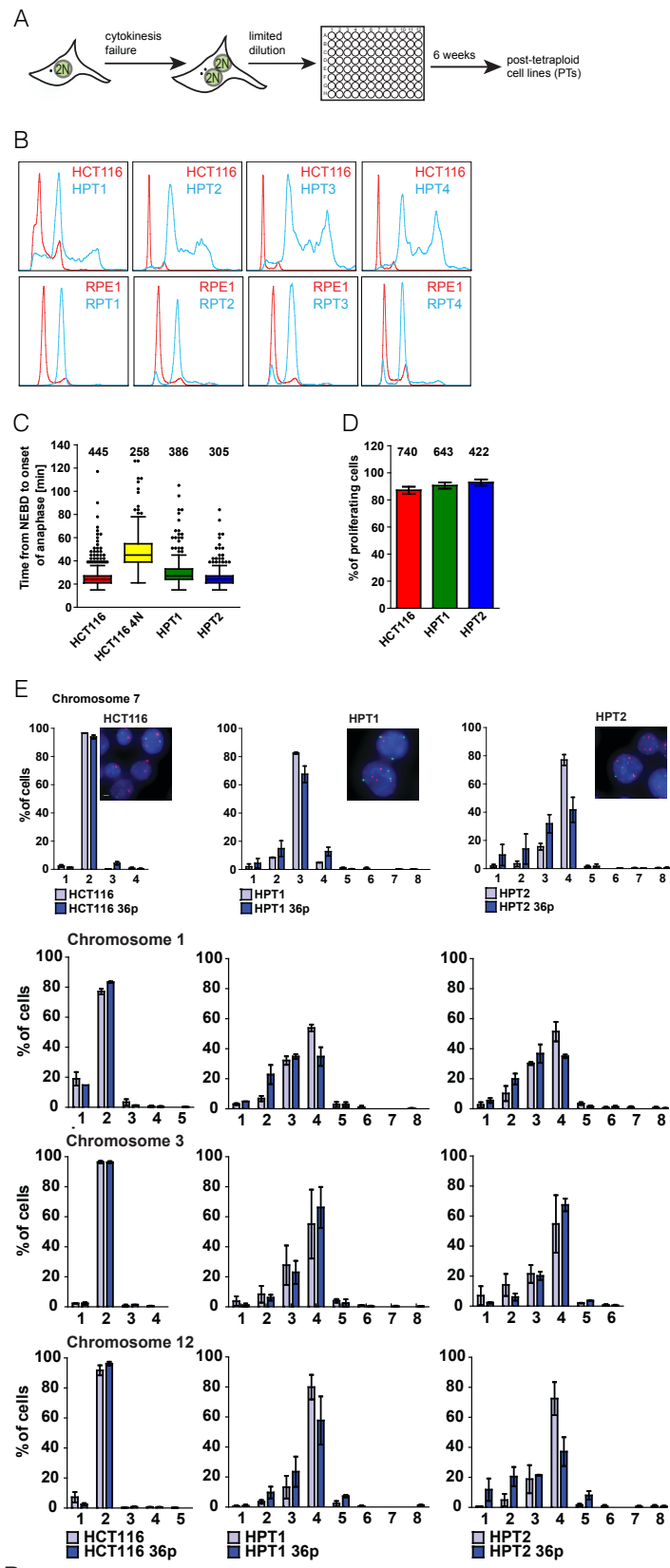


Fig. 2: Generation and characterization of post-tetraploid (PT) cell lines. **A** Depiction of the generation process of PTs. **B** DNA content profiles by flow cytometry after propidium iodide staining of HPTs (top row) and RPTs (bottom row). **C** Time spent in mitosis measured from nuclear envelope breakdown (NEBD) to onset of anaphase (OA) in HCT116 and its PTs measured by live cell imaging in four independent experiments. Tukey range and median are plotted **D** Numbers of proliferating cells (cells undergoing at least two mitoses during time lapse image acquisition) in HCT116 and its PTs measured by live cell imaging in four independent experiments. Mean and standard deviation plotted **E** Chromosome numbers assessed via interphase FISH in early and late passages of HCT116 and its PTs in two independent experiments. Mean and standard error of the mean (SEM) plotted. Data and figures from Kuznetsova (2013)

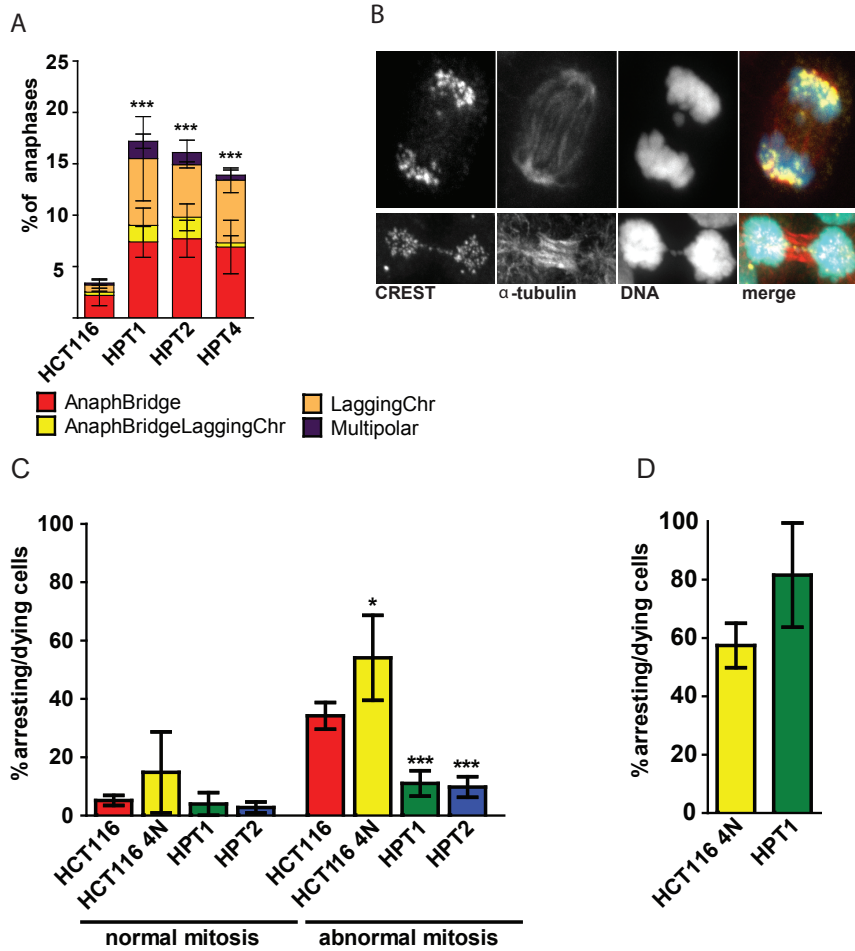


Fig. 3: Survival of PTs after mitotic errors. **A** Depiction of the percentage of phenotypes of mitotic errors (anaphase bridges, lagging chromosomes, both or multipolar errors) in all cell lines assessed in 20x magnified images with Sytox Green DNA staining for HCT116 and HPTs. Mean and standard deviation (SD) of three independent experiments **B** Depiction of lagging chromosomes (top) and anaphase bridges (bottom) at 64x magnification stained with CREST (centromeric staining), α -tubulin (microtubule staining) and DNA staining. **C** Percentage of cells arresting or dying in all cell lines after normal or abnormal (bipolar) mitosis assessed by live-cell imaging. Mean of four independent experiments and SD are plotted. Unpaired Student t-test **D** Percentage of cells arresting or dying in all cell lines after multipolar mitosis. Mean of four independent experiments and SD are plotted. Data and figures from Kuznetsova (2013). Significance levels: * denotes $p \leq 0.05$, ** denotes $p \leq 0.01$, *** denotes $p \leq 0.001$

tion and regulatory domain. It regulates cell cycle arrest, DNA repair and apoptosis among others (Bullock and Fersht, 2001). p53 gets activated by cellular stress such as DNA damage, inflammation, hypoxia and viral infection (Banin, 1998; Hirao, 2000; Shieh et al., 1997; Hofseth et al., 2003; Graeber et al., 1994; Lowe and Ruley, 1993). In case of stress, p53 gets transported into the nucleus after p53 tetramerization (Trostel et al., 2006). After oligomerization, p53 associates with dynein (Giannakakou et al., 2000). Dynein itself is a motor protein moving along microtubules from their plus to minus ends, i.e. from the cell periphery to the center (Schnapp and Reese, 1989; Hirokawa, 1998). p53 gets transported by dynein along the microtubules to the nucleus, which is in close proximity to the centrosome (Burakov and Nadezhina, 2013; Moll et al., 1996). p53 gets transported through the nuclear pore by importin- α (Kim et al.,

2000) (for review: Maki (2010)).

p53 is mutated in up to 70% of cancer patients depending on the cancer-type (Brosh and Rotter, 2009; Rivlin et al., 2011)). In a recent study on bladder cancer, an inactivation of TP53 was reported in 76% of samples (The Cancer Genome Atlas Research Network, 2014). p53 inactivation in non-germline mutations is achieved predominantly by missense mutations in the DBD of p53 and impairs the ability of p53 to bind DNA in order to activate transcription of downstream targets. Interestingly, one mutant allele is sufficient to perturb p53 function since p53 relies on a tetrameric state for activation, which is disturbed by the mutant p53 allele, i.e. p53 is haploinsufficient. Additionally, this mutant state is followed in many cases by loss of heterozygosity (LOH) where the wildtype allele gets deleted or mutated (Rivlin et al., 2011). The importance of undisturbed p53 function becomes clear in light of the Li-Fraumeni Syndrome which is caused by a germline mutation of TP53 and predisposes patients to a wide variety of tumor-types (Malkin et al., 1990; Varley, 2003; Brosh and Rotter, 2009). Furthermore, mutant p53 is associated with oncogenic gain-of-function mutations such as drug resistance and apoptotic interference (Brosh and Rotter, 2009). p53 cellular stabilization and activation are regulated by its post-translational modifications that can influence for example the binding of Mdm2 to p53 (Feng et al., 2005) (for review: Toledo and Wahl (2006)). Serine 15 of p53 is phosphorylated by many different kinases, such as ATM, ATR, DNA-PK and p38 upon DNA damage (Banin, 1998; Tibbetts et al., 1999; Shieh et al., 1997; Bulavin et al., 1999; Vitale et al., 2008; She et al., 2000) (for review: Toledo and Wahl (2006)). ATM, for example, gets activated by oxidative stress and canonical DNA damage (Guo et al., 2010; Janssen et al., 2011). Oxidative stress is caused by environmental or internal influences that can lead to oxidative DNA damage such as base lesions (Cooke et al., 2003). The stress kinase p38 gets activated in response to cellular stress signals such as disruption of the cytoskeleton and upon missegregation (Mikule et al., 2006; Thompson and Compton, 2010). Additionally, upon cellular stress p38 directly phosphorylates p53 at many different serine residues including serine 15 (Bulavin et al., 1999; She et al., 2000). Additionally, p53 is phosphorylated at serine 15 upon chromosome missegregation in freshly arising tetraploids (Kuffer et al., 2013).

To identify the molecular mechanisms and pinpoint protein candidates involved in the survival of post-tetraploid cells and their tolerance to mitotic errors, gene expression patterns of two independent post-tetraploid clones derived from HCT116 were analyzed in our lab using microarrays as an initial approach. The analysis revealed deregulation of the p53 pathway. In particular, remarkable changes were observed for CDKN1A (\log_2 0.9 increase of mRNA levels in one post-tetraploid cell line out of two, namely HPT2) and MDM2 genes (\log_2 increase of

0.8 for both analyzed post-tetraploid cell lines, namely HPT1 and 1.9 for HPT2), encoding p21 and Mdm2, respectively (personal communication Milena Dürrbaum). Mdm2 is an E3 ligase responsible for p53 ubiquitination at the C-terminal lysines and subsequent degradation. It is the cellular antagonist of p53 and the product of a p53-inducible gene which ensures low p53 levels by an autoregulatory negative feedback loop (Moll and Petrenko, 2003). p21 is a cyclin-dependent kinase inhibitor, which activates cell cycle checkpoints in response to DNA damage and therefore maintains genetic fidelity in eukaryotic cells (El-Deiry et al., 1993; Deng et al., 1995). Interestingly, p21 nuclear turnover is influenced by Mdm2, the p53 antagonist, in an ubiquitin-independent manner (Jin et al., 2003) (for review: Warfel and El-Deiry (2013)). The observed changes might suggest direct involvement of the p53 pathway in the tolerance to mitotic errors in post-tetraploid progeny.

The aim of this thesis is to characterize RPTs with respect to aneuploidy and CIN and the identification of the molecular mechanism which allows the survival of PTs after mitotic errors. Characterizing RPTs is very important since they are derived from a non-cancerous, immortalized cell line in comparison to HPTs, which are derived from a cancerous cell line. Having characterized both cell lines is essential to validating prospective results on the mechanism of tolerance to chromosome missegregation. To achieve this, RPTs will be analyzed by an interphase Fluorescence *In Situ* Hybridization (FISH) experiment on early and late passages to assess their chromosome copy numbers and to detect potential changes in between the passages. Additionally, a copy number analysis performed in collaboration with the Kloostermann lab will be added to the results of the FISH experiments.

As a second part, I want to find the molecular mechanism leading to tolerance to chromosome missegregation in both HPTs and RPTs. Since it is known that the p53 pathway is involved in tolerance to missegregation I tested the nuclear p53 levels after micronucleation in RPTs. Next I investigated whether activation of p53 upon induced missegregation with a Vs83-washout is impaired. I assessed the abundance of p53 and pSer15-p53 by western blotting. Since we could not observe a link between induced missegregation and impaired p53 activation, we wanted to know what other cellular stress results in p53 activation. DNA damage is one of the cellular stress signal to which p53 responds. I assessed the levels of p53, pSer15-p53, p38 and pThr180Tyr182-p38 with western blotting experiments after induced DNA damage. Since tetraploidization can be an intermediate route to aneuploidy, CIN and eventually tumorigenesis, understanding of the molecular mechanism leading to tolerance to missegregation in tetraploids could enable us to prevent tumorigenesis in the long run.

4 Results

4.1 Characterization of RPE1 derived post-tetraploids (RPTs)

Previous work of a postdoctoral student in our laboratory, Anastasia Kuznetsova, showed that HCT116 derived post-tetraploids (HPTs) display aneuploidy and CIN (Fig. 2 E). HPTs had variable karyotypes with median chromosome numbers between near-triploid and near-tetraploid. This shows that HPTs have numerical aneuploidy (Kuznetsova, 2013). Whether HPTs also show a considerable CIN phenotype was assessed by evaluation of chromosome numbers in interphase Fluorescence *In Situ* Hybridization (FISH) experiments for chromosomes 1, 3, 7 and 12 in early and late (36) passages (Fig. 2 E). FISH is a method, which allows determination of the copy number of chromosomes in single cells with the help of fluorescently labeled centromeric probes. HPT1 and HPT2 showed a tendency towards loss of chromosomes and displayed ongoing changes in their copy number between early and late passages. Additionally, chromosomal instability manifested itself through an increase in mitotic errors. About 15% of HPT cells showed mitotic errors, such as anaphase bridges, lagging chromosomes and multipolar mitosis. Their parental cell line, HCT116, in comparison showed mitotic errors only in less than 5% of cells (Fig. 3 A). Since post-tetraploids were derived by a single tetraploidization event, this means that tetraploidization can result in aneuploidy and CIN (Kuznetsova, 2013). To ensure that changes in mitosis in HPTs and the marked difference from the parental cell line HCT116 are not due to the fact that HCT116 is a transformed cell line, I performed similar experiments with RPT cell lines that were derived by tetraploidization from the immortalized, non-transformed cell line RPE1.

To rule out that experimental data is compromised by external sources, I checked all used cell lines for a potential mycoplasm infection with the MycoTrace kit. This kit can detect various mycoplasm strains. None of the cell lines were infected (Fig. S1).

The RPE1 derived post-tetraploids (RPTs) were analyzed in early and late passages (0 and 12 passages, respectively) in an interphase FISH experiment of chromosomes 3 and 7.

In previous work, karyotyping of metaphase spreads showed that RPTs range from near-diploid to near-tetraploid (Kuznetsova, 2013). Like HPTs, all RPTs were aneuploid which suggests that the evolution of cells into aneuploid cells obtained by one tetraploidization event is not dependent on the parental cell line, cancerous or not.

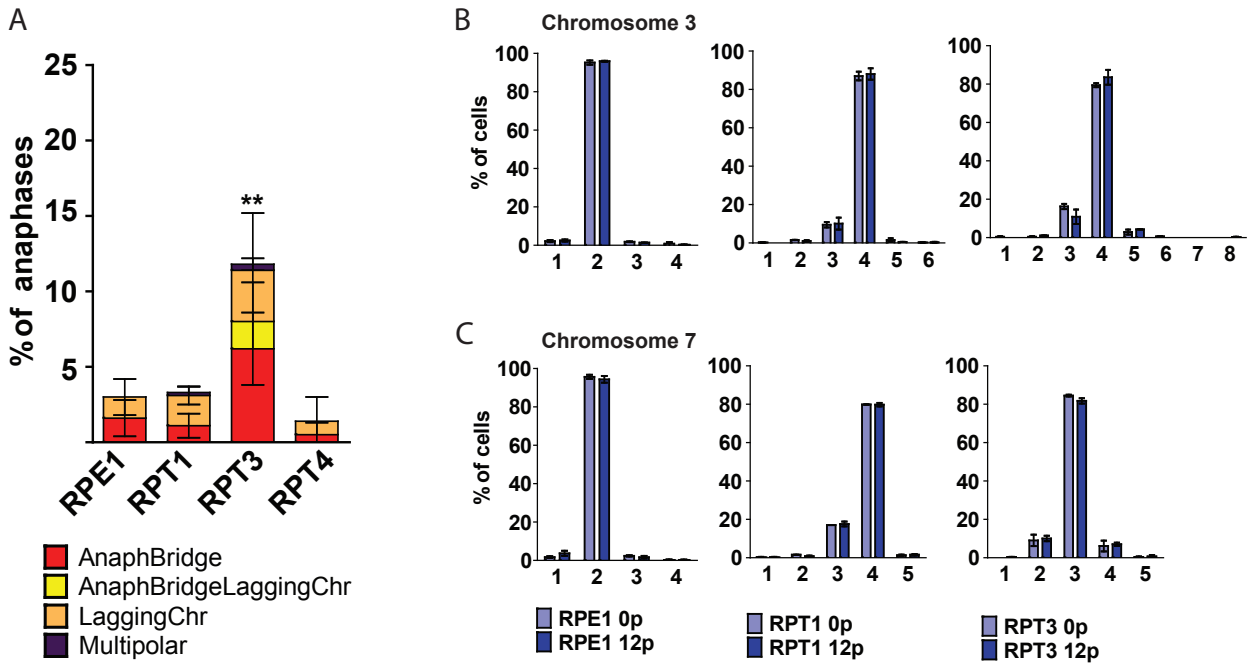
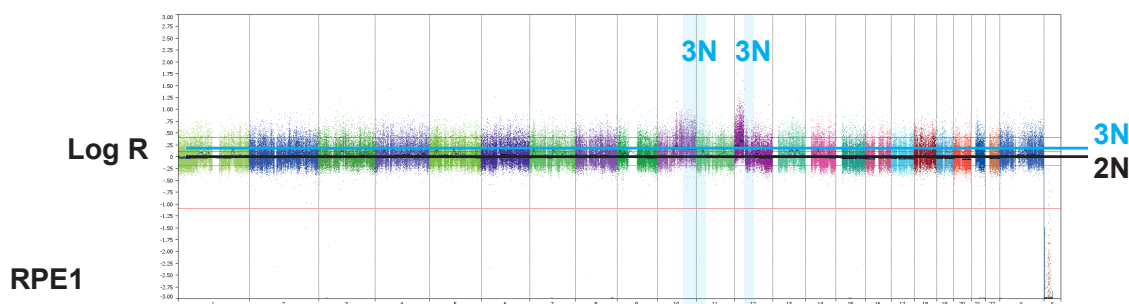


Fig. 4: Characterization of post-tetraploid cell lines derived from RPE1. **A** Depiction of the percentage of phenotypes of mitotic errors (anaphase bridges, lagging chromosomes, both or multipolar errors) in all cell lines. Assessed in 20x magnified images with Sytox Green DNA staining for RPE1 and RPTs. Mean of three independent experiments and SD are plotted. **B** FISH data of centromeric regions of chromosome 3 in the cell lines RPE1, RPT1 and RPT3 in early (0) and late (12) passages depicted as percentage of cells with a certain chromosome number in mean and SEM of two independent FISH experiments **C** FISH data of centromeric regions of chromosome 7 in the cell lines RPE1, RPT1 and RPT3 in early (0) and late (12) passages depicted as percentage of cells with a certain chromosome number in mean and SEM of two independent FISH experiments. Significance levels: * denotes $p \leq 0.05$, ** denotes $p \leq 0.01$, *** denotes $p \leq 0.001$

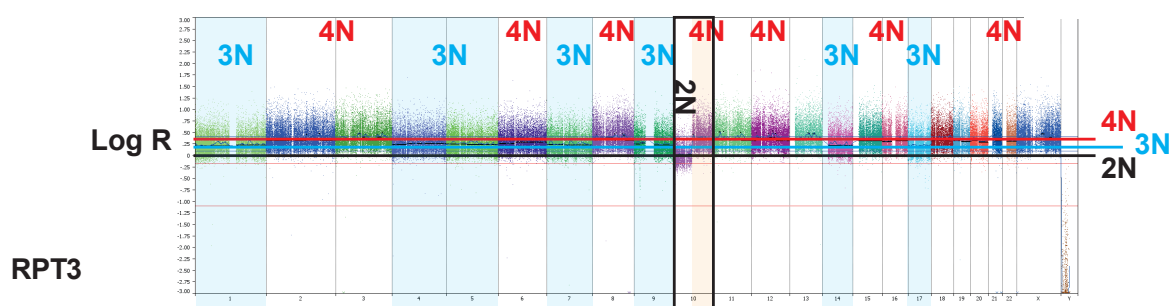
To investigate if RPTs harbor mitotic errors with increased frequency similar to HPTs, mitotic abnormalities in anaphase were analyzed by Sytox Green stained fixed cell imaging. The parental cell line RPE1 showed less than 5% of cells displaying mitotic errors. RPT1 and RPT4 showed similar and slightly less frequent mitotic errors than RPE1. In contrast to that, about 12% of cells displayed mitotic errors in RPT3. The mitotic errors mostly consisted of anaphase bridges and lagging chromosomes and only to a minor fraction of multipolar errors (Fig. 4 A). Since RPT1 and RPT4 did not show increased frequencies of mitotic errors, they are most likely chromosomally stable.

To address the question whether RPTs, particularly RPT3, display CIN and to support the karyotyping data, I performed two independent FISH experiments for each of the cell lines RPE1, RPT1 and RPT3 with centromeric probes against chromosomes 3 and 7. RPE1 almost exclusively showed two sets of chromosomes 3 and 7 with almost no changes between the early and late passages (Fig. 4 B, C). This was to be expected since RPE1 is known as a stable

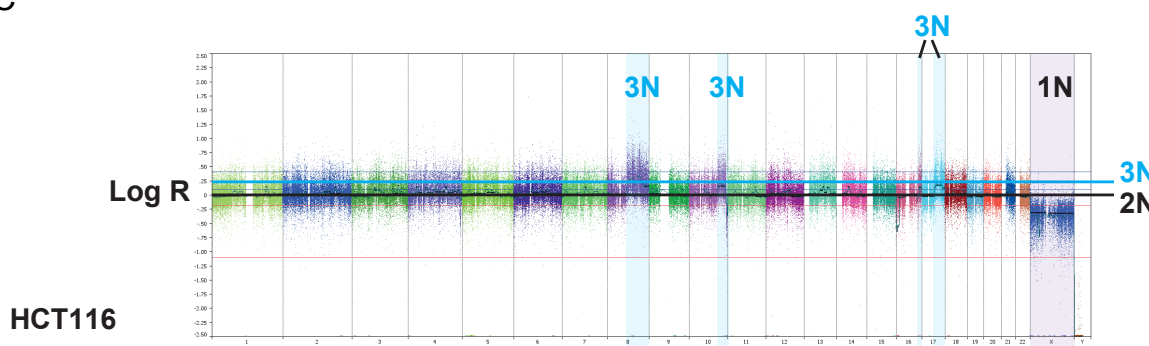
A



B



C



D

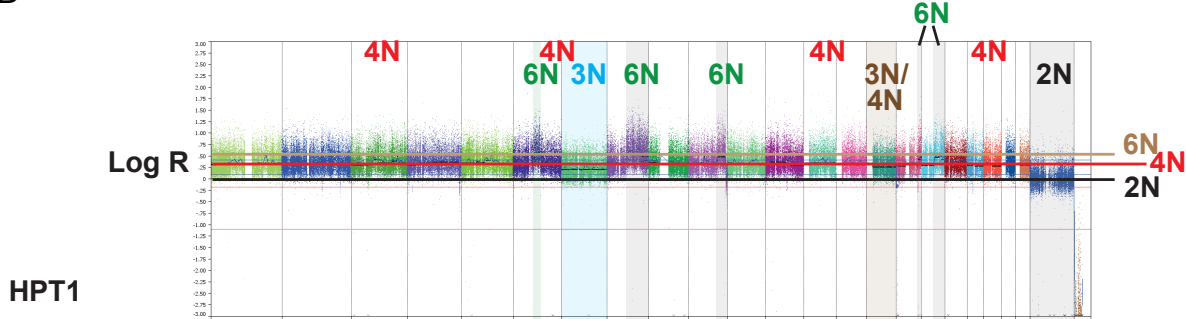


Fig. 5: Copy number analysis of HCT116, HPT1, RPE1 and RPT3 by SNParray data. Done in collaboration with Kloosterman, W.P., Uni Utrecht, NL. Copy number analysis for **A** RPE1 **B** RPT3 **C** HCT116 **D** HPT1. Significance levels: * denotes $p \leq 0.05$, ** denotes $p \leq 0.01$, *** denotes $p \leq 0.001$

diploid cell line (<http://www.lgcstandards-atcc.org/Products/All/CRL-4000.aspx>; Thompson and Compton (2008)). In contrast to that, RPT1 and RPT3 showed mainly four copies of chromosome 3 with more variations in the chromosome numbers compared to RPE1 and with a bias towards chromosome loss. For example, in both tested RPTs about 20% of cells contained three copies of chromosome 3, whereas the occurrence of more than four copies of chromosome 3 was very low. Chromosome 7 was present in four copies in most RPT1 cells. However, approximately 20% of cells contained only three copies of chromosome 7 and a very small fraction showed chromosome numbers from one to five. RPT3 showed a major fraction of cells with three copies of chromosome 7 (about 80%) in both early and late passages. It showed approximately 10% of cells with either 2 or 4 copies of chromosome 7. Both RPT1 and RPT3 showed numerical aneuploidy with a bias towards chromosome loss but only minor changes in chromosome number between early and late passages. Thus, FISH analysis revealed that post-tetraploid cell lines derived from the non-cancerous cell line RPE1 can become aneuploid.

Next I wanted to see whether both HPTs and RPTs show copy number variations compared to their respective parental cell lines.

The copy number variation analysis by SNParray data, which is population-based, showed that almost all chromosomes are present in two copies in RPE1. Small parts of chromosomes 10 and 12 were present in 3 copies instead of two (Fig. 5 A, blue bars). Furthermore, the cell line RPE1 did not possess a Y-chromosome. These results confirm that RPE1 is a stable, diploid cell line derived of female origin (<http://www.lgcstandards-atcc.org/Products/All/CRL-4000.aspx>).

RPT3 (Fig. 5 B) differed markedly from RPE1. Each chromosome should be present in twice the number compared to RPE1 assuming that RPT3 cells are chromosomally stable since RPTs were derived by an aborted cytokinesis of the RPE1 cell line. For example, chromosome 10 was present partly in two and partly in four copies (Fig. 5 B; black box). However, if it would have the same copy number variations as RPE1, the part of chromosome 10 that was present in three copies in RPE1 should be present in six copies in the post-tetraploid RPT3. The same holds true for chromosome 12, which did not maintain the copy number variation of the parental cell line. Chromosome 12 was present exclusively in four copies in RPT3. Since part of chromosome 12 was present in three and the rest in two copies in RPE1, this variation should have been mirrored in RPT3, assuming that the karyotype should not change.

Furthermore, RPT3 showed a trend towards loss of chromosomes since not only chromosome 7 but various other chromosomes were present in three copies instead of four (Chromosomes 1, 4, 5, 9, 14, 17). The loss of chromosome 7 was already shown in the FISH experiment (Fig. 4 B,

C). RPT3 showed severe aneuploidy with a bias towards chromosome loss. Additionally, it did not display the same copy number variations as RPE1.

A strong aneuploid phenotype was not observed in other RPE1 derived clones (Fig. S2). RPT1 and RPT4 still share the copy number variation of part of chromosome 10 of their parental cell line and are tetraploid for most chromosomes.

Most chromosomes of the diploid cell line HCT116 were present in two copies (Fig. 5 C). Parts of chromosomes 8, 10, 16 and 17 were present in three copies. The X-chromosome was present in one copy, whereas the Y-chromosome was completely absent. This was to be expected since HCT116 is described as a stable, near-diploid cell line (Thompson and Compton, 2008) with gains in bigger arms of chromosomes 8, 10 and 17 as well as amplifications in the terminal region of the long arm of chromosome 16 (16qter). Furthermore, HCT116 is described to contain one copy of the X-chromosome and in metaphase spreads only 16% of cells had a Y-chromosome(Masramon et al., 2000). The Y-chromosome could therefore not be seen in a population based analysis.

The copy number variations of HCT116 on chromosomes 8, 10, 16 and 17 were observed in HPT1, as well (Fig. 5 D; marked in grey). However, HPT1 had obtained additional copy number variations apart from the ones that were already present in the parental cell line HCT116. Chromosome 7 was present in three copies which was already observed in FISH experiments (Fig. 2 E, Kuznetsova (2013)). Furthermore, part of chromosome 6 was present in 6 copies and chromosome 15 was present in three or four copies in part of the population. To sum up, HPT1 is aneuploid but does not show the same observed bias of HPTs and RPT3 towards chromosome loss.

HPT6 showed copy number variations on chromosomes 8, 10 and 17 and had additionally lost one copy of chromosome 11 and 13 (Fig. S2). Therefore, both HPT1 and HPT6 are aneuploid and show a slight tendency towards chromosome loss.

4.2 Accumulation of nuclear p53 upon missegregation in PTs

Fresh tetraploids display increased frequencies of bipolar and multipolar mitotic errors and arrest or die in a p53-dependent manner (Kuffer et al., 2013). During generation, post-tetraploids display a low recovery efficiency of approximately 1%. This suggests that the majority of tetraploid cells arrest or die due to p53 activation (Andreassen et al., 2001; Fujiwara et al., 2005; Vitale et al., 2010). Additionally, HPTs are able to proliferate after missegregation during bipolar mitosis in a higher percentage than their parental cell line (Fig. 3 C, Kuznetsova

(2013)). This suggests a deregulation in p53 upon tetraploidization and missegregation in post-tetraploids. This claim is supported by data from our laboratory showing that in HPTs the expression of members of the p53 pathway, e.g. Mdm2 and p21, is deregulated (personal communication Milena Dürrbaum). Additionally, it was shown previously for HPTs by A. Kuznetsova, that they have an attenuated nuclear p53 enrichment upon micronucleation (Fig. 6 A, Kuznetsova (2013)).

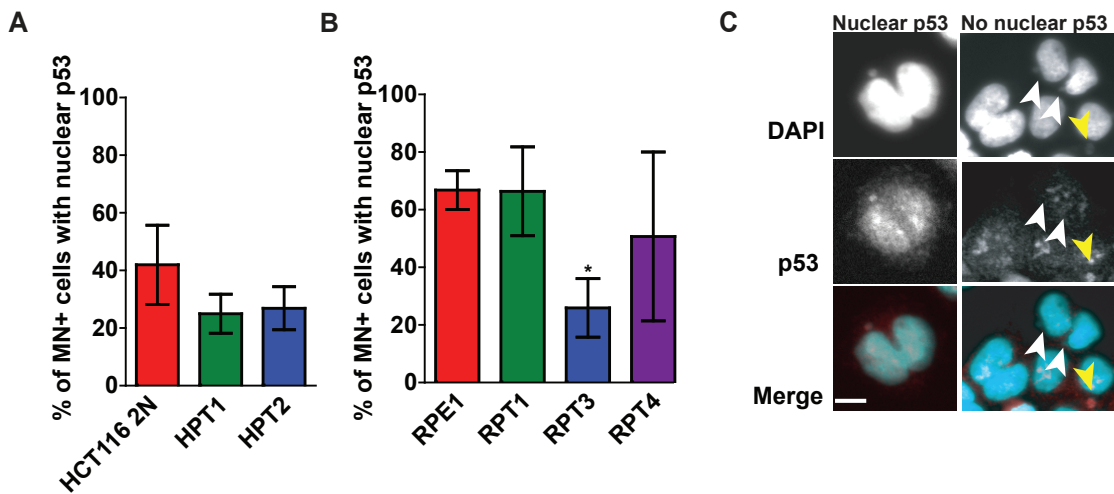


Fig. 6: Post-tetraploids deregulate the p53 signaling pathway. Accumulation of p53 in the nucleus of cells with micronuclei in **A** HCT116 and HPTs. Accumulation was determined by visual inspection. The mean and SEM of four independent experiments are plotted. Data from Anastasia Kuznetsova. **B** RPE1 and RPTs. Accumulation was determined by automated cell profiler analysis. The mean and SEM of four independent experiments are plotted. **C** Representative images of p53 accumulation in the nucleus and micronuclei in micronucleated cells. Yellow arrowheads: micronucleus with enriched p53 signal, white arrowheads: no p53 enrichment in the micronucleus, bar: 10 μ m reference length. Data and figure from (Kuznetsova, 2013). Significance levels: * denotes $p \leq 0.05$, ** denotes $p \leq 0.01$, *** denotes $p \leq 0.001$

Therefore it was important to investigate whether missegregation in cell lines derived from the non-cancerous RPE1 would alter the p53 signal, too. Alterations of p53 upon missegregation were tested with a micronucleation assay. In this assay, cells are subjected to a DCD washout. Since DCD inhibits cytokinesis thus leading to tetraploidization, cells that underwent mitosis contain two nuclei in the first cell cycle after the abortive cell division. The population of binucleated cells was analyzed for the presence of micronuclei. Micronuclei are formed as a consequence of chromosome missegregation, i.e. when whole chromosomes or part of chromosomes are not segregated properly (Crasta et al., 2012).

It was shown previously by A. Kuznetsova that in the cell lines HPT1 and HPT2 only approximately 25% of cells enrich nuclear p53 compared to about 40% for HCT116 after chromosome segregation errors (Fig. 6 A, Kuznetsova (2013)). In RPTs, only the cell line RPT3 showed a

significant lower number of micronucleated cells with enriched nuclear p53 (about 30%) compared to RPE1. RPT1 and RPT4 displayed a similar percentage of micronucleated cells as RPE1 (about 60%) (Fig. 6 B).

To sum up, all post-tetraploids derived from the cancerous cell line HCT116 showed attenuated nuclear p53 enrichment, whereas only RPT3 of all the post-tetraploids derived by the non-cancerous, immortalized cell line RPE1 displayed this attenuation.

4.3 Changes in the abundance of p53 in post-tetraploids after induced missegregation

Since the accumulation of nuclear p53 is attenuated in missegregating post-tetraploids, it is interesting to investigate whether the abundance of p53 and p53 that is phosphorylated on serine 15 (called pSer15-p53 in the following) is changed upon induced missegregation. p53 gets activated by phosphorylation which protects it from degradation (Moll and Petrenko, 2003). It is known that the abundance of phosphorylated p53 increases after tetraploidization in fresh tetraploids (Kuffer et al., 2013).

To test whether the activation of p53 by phosphorylation of serine 15 is altered in post-tetraploids, I induced missegregation via a Vs83-washout strategy, which prevents duplicated centrosomes from moving to the cell poles by inhibiting the kinesin motor-protein eg5 until the drug is washed out. During the drug treatment, erroneous kinetochore-microtubule attachments arise from monopolar spindles, so-called monoasters, which cannot get resolved in a timely manner (Müller et al., 2007). After the drug is washed out, the centrosomes are able to move to the poles. This leads to errors in chromosome segregation.

In order to make sure that I could use the Vs83-washout in a population based approach, such as immunoblotting, I recorded live-cell imaging data for seven hours directly after the washout. This enables me to control the effect of the drug treatment on HCT116 and all HPTs. A population based approach can only be used if the cell lines react similarly to the drug washout.

I found three different phenotypes of missegregation: no missegregation, "mild" missegregation, such as lagging chromosomes and anaphase bridges, which could also be seen in untreated samples, and "severe" missegregation where a major part of DNA gets missegregated (Fig. 7 A). Results from two independent experiments suggest a similar frequency of all mitotic phenotypes in all analyzed cell lines. Thus, the Vs83-washout strategy is suitable for testing the effect of

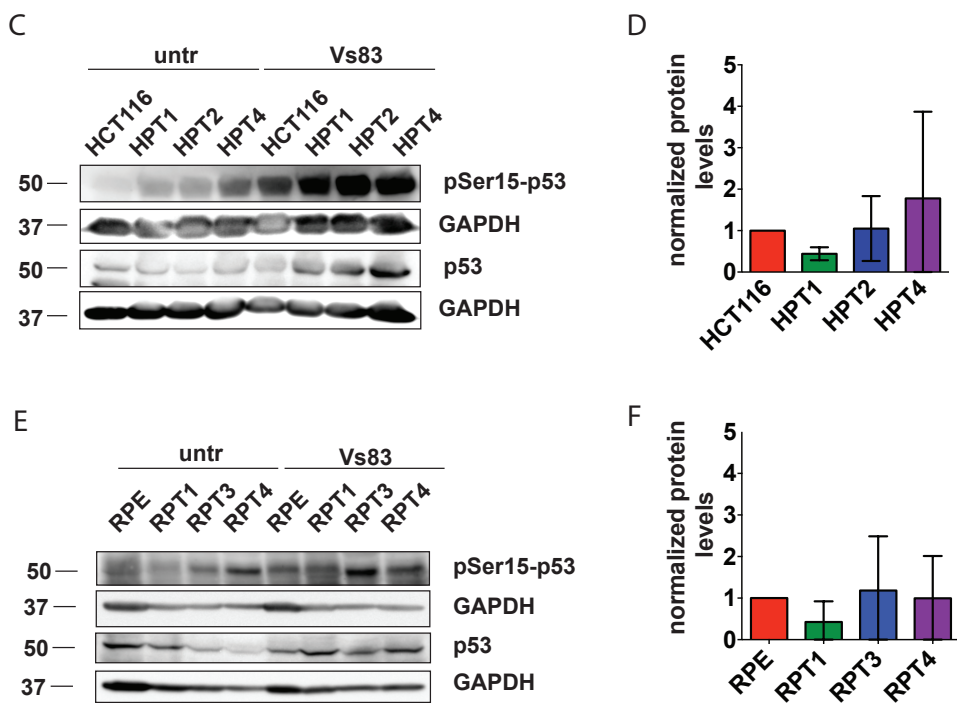
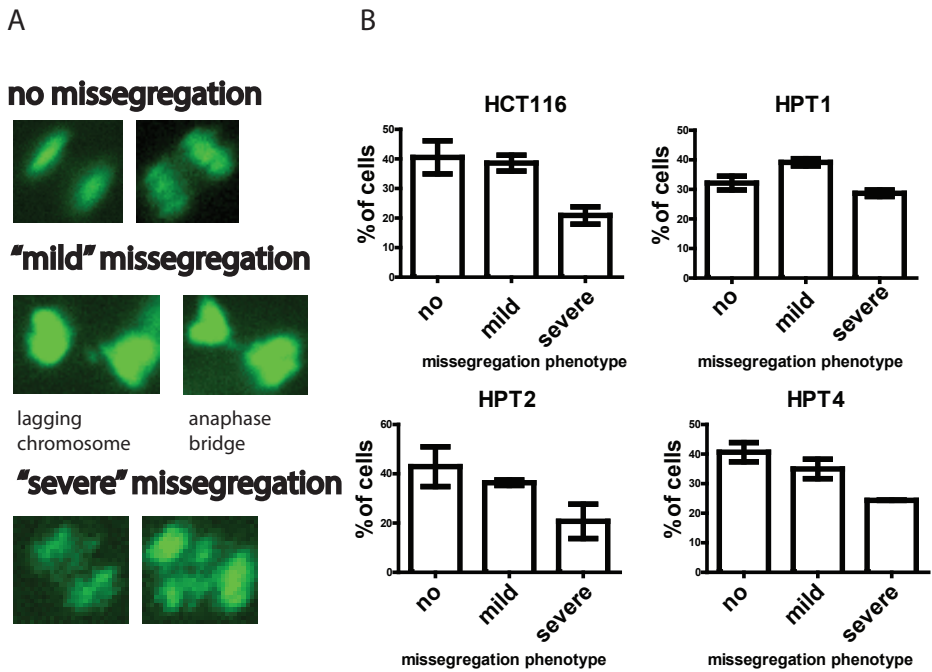


Fig. 7: Activation of p53 after Vs83-induced missegregation. **A** Representative images of the possible missegregation phenotypes: no missegregation (top), "mild" missegregation (middle) and "severe" missegregation assessed via live-cell imaging (green: H2B-GFP signal). **B** Percentage of cells with missegregation phenotypes in HCT116, HPT1, HPT2 and HPT4 from two independent experiments. Mean and SD are plotted. **C** Representative western blot for untreated and treated (Vs83-washout) HCT116 and HPT cell lines. **D** Western blot results of four independent experiments after Vs83-induced missegregation. Calculation of pSer15-p53/p53 ratio in HCT116 and HPT cell lines after induced missegregation. Western blot results were normalized to respective loading control (GAPDH or ponceau) first, followed by a normalization to HCT116. **E** Representative Western blot for untreated and treated (Vs83-washout) RPE1 and RPT cell lines. **F** Western blot results of three independent experiments after Vs83-induced missegregation. Calculation of pSer15-p53/p53 status in RPE1 and RPT cell lines after induced missegregation. Western results were normalized to respective loading control (GAPDH or ponceau) first, followed by a normalization to RPE1. Mean and SEM are plotted in D and F.

induced missegregation on the p53 pathway by western blotting (Fig. 7 B).

The blots from HCT116 and the HPTs showed a stronger pSer15-p53 and p53 signal in Vs83-treated samples compared to the untreated samples (Fig. 7 C). The blots from RPE1 and the RPTs showed an increase in pSer15-p53 and p53 in Vs83-treated samples compared to untreated samples, as well (Fig. 7 E).

When I analyzed the pSer15-p53/p53 ratio in HCT116 and HPTs, I found that all HPTs behaved similar to HCT116. The only exception was HPT1 where a slight reduction in the pSer15-p53/p53 ratio was observed (normalized protein levels of about 0.5) (Fig. 7 D). All RPTs showed a pSer15-p53/p53 ratio similar to RPE1, as well (Fig. 7 F).

Taken together, neither HPTs nor RPTs showed a decrease in the pSer15-p53/p53 ratio upon induced missegregation compared to their respective parental cell lines.

4.4 Changes in the abundance of p53 and p38 in post-tetraploids upon induced DNA damage

Since I could not detect a link between induced missegregation and impaired p53 activation in HPTs nor RPTs, I was interested under what circumstances p53 activation might be impaired in PTs. p53 is involved in the response to DNA damage (Banin, 1998; Moll and Petrenko, 2003; Toledo and Wahl, 2006; Shaltiel et al., 2014) and it becomes phosphorylated at serine 15 by many different kinases, such as p38, ATM and ATR (Toledo and Wahl, 2006; Tibbetts et al., 1999).

To test whether p53 activation is impaired in response to DNA damage, I performed immunoblotting experiments against pSer15-p53 and p53 in untreated and doxorubicine (DRB) treated cells. DRB is a DNA damaging reagent and induces DNA single and double strand breaks by blocking the activity of DNA topoisomerase II (Tewey et al., 1984). The abundance of pSer15-p53 and p53 was determined for HPTs and RPTs, their diploid parental cell lines, as well as newly formed tetraploids of the parental cell lines (Fig. 8 C, F).

The parental diploid cell line HCT116 was used as a normalization reference with a ratio of pSer15-p53/p53 of 1.0. The response to DNA damage, which is represented by the ratio of phosphorylated p53 over total p53, was decreased in HPT2 and HPT4 to 0.1 and 0.3, respectively. The decrease in the ratio of pSer15-p53/p53 in HPT2 was significant. HPT1 and freshly tetraploid HCT116 did not show deregulated p53 signaling under DNA damaging conditions (Fig. 8 B, normalized protein levels of 0.8 and 0.7, respectively).

All RPTs showed a decreased pSer15-p53/p53 ratio (normalized protein levels of about 0.3 to

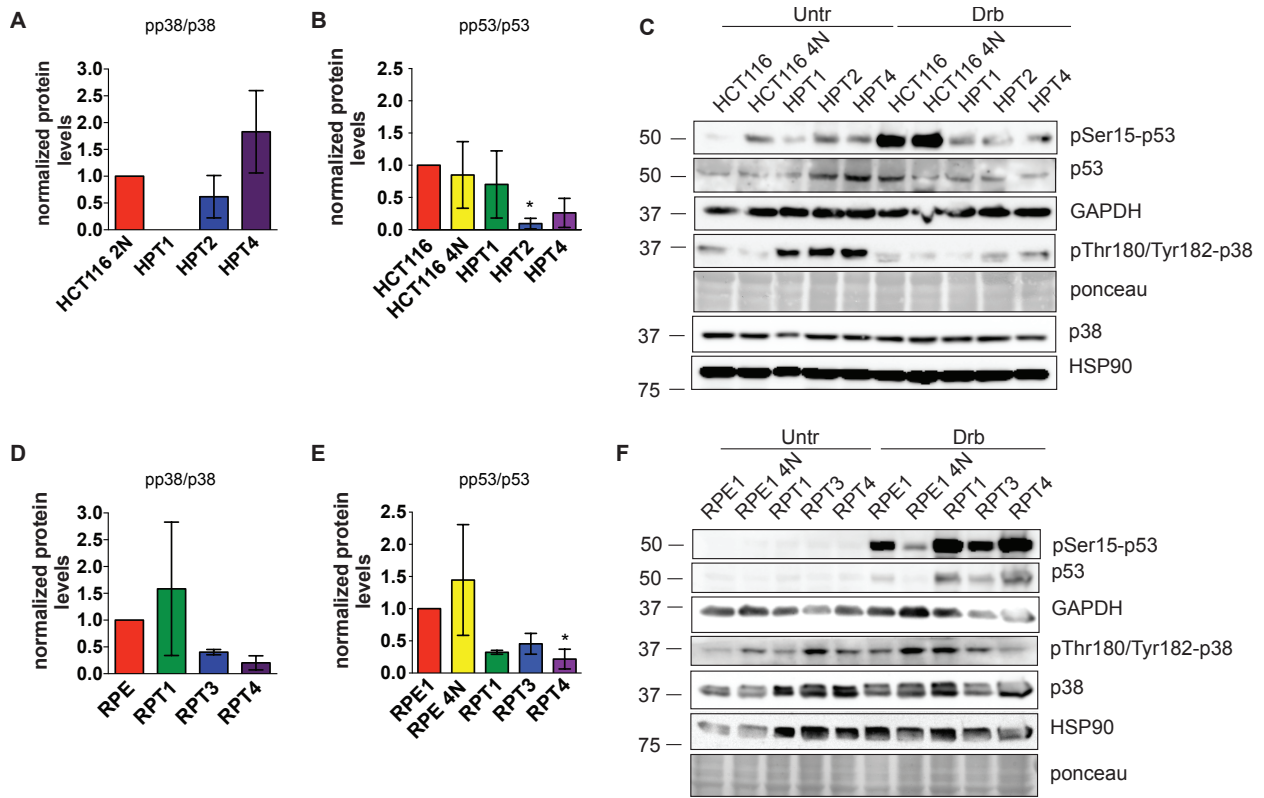


Fig. 8: Post-tetraploids deregulate the p53 signaling pathway upon induced DNA damage. Calculation from western blot results of at least two independent experiments after induced DNA damage with doxorubicine (DRB). Western blot results were normalized to a respective loading control first, followed by a normalization to the respective diploid parental cell line (HCT116 or RPE1). pSer15-p53 and pThr180/Tyr182-p38 were normalized by ponceau as a loading control, p53 was normalized to GAPDH as a loading control and p38 was normalized to HSP90 as a loading control. **A** Calculation of pThr180/Tyr182-p38/p38 ratio in HCT116 and HPT cell lines. Mean and SD are plotted **B** Calculation of pSer15-p53/p53 ratio in HCT116 and HPT cell lines. Mean and SEM are plotted **C** Representative Western blot for HCT116 and HPT cell lines, immunoblotting against p38 and HSP90 performed by Katarzyna Seget. **D** Calculation of pThr180/Tyr182-p38/p38 ratio in RPE1 and RPT cell lines. Mean and SEM are plotted. **E** Calculation of pSer15-p53/p53 ratio in RPE1 and RPT cell lines. Mean and SEM are plotted **F** Representative Western blot for RPE1 and RPT cell lines. Ordinary one-way ANOVA compared to parental cell lines for graphs A, B, D and E. Significance level: * denotes $p \leq 0.05$

0.4) in DRB treated samples compared to their parental cell line RPE1 (normalized reference level of 1.0). The decrease in RPT4 was significant. The newly tetraploid RPE1 cell line did not show a decrease in the p53 response (normalized protein levels of 1.4; Fig. 8 E). In summary, the ratio of pSer15-p53/p53 was decreased for HPT2, HPT4 and all of the RPTs.

Since the phosphorylation of p53 seems to be altered in HPT2, HPT4 and all RPTs, I tested whether the upstream activation of p53 might be altered thus possibly causing the change in p53 activation. p53 gets phosphorylated at serine 15 by many different kinases (Toledo and Wahl, 2006). p38 seems a reasonable candidate of an upstream p53 activator since p38 is not only phosphorylating serine 15 of p53 directly (She et al., 2000) but is responsible for the translation of p21, a downstream target of p53, as well (Kumari et al., 2013). Moreover, p38 is also

associated with the activation of p53 after chromosome missegregation (Thompson and Comp-ton, 2010). To investigate the behavior of p38, the samples of the DRB experiment described above were used in western blots against p38 and phosphorylated p38 (pThr180/Tyr182-p38) for all HPTs and RPTs, as well as their respective parental cell lines.

The phosphorylated form of p38 seems to be less abundant in western blots for HPTs in treated compared to the untreated samples (Fig. 8 C). For RPTs, a decrease was only visible in RPT3 and RPT4 in DRB treated samples compared to untreated samples (Fig. 8 D). The abundance of p38 is the same throughout all samples and treatments for both HPTs and RPTs (Fig. 8 C, F).

Analogously to p53, I tested whether the ratio of phosphorylated p38 over total p38 was altered upon DRB-induced DNA damage. For HPTs, only HPT1 had a clearly visible decreased ratio of pThr180/Tyr182-p38/p38 (normalized protein level of about zero) compared to the parental cell line HCT116 (Fig. 8 D, normalized protein level of 1.0). HPT2 and HPT4 had a pThr180/Tyr182-p38/p38 ratio comparable to the parental cell line with normalized protein levels of approximately 0.6 and 2.0, respectively.

RPT3 and RPT4 showed a decreased pThr180/Tyr182-p38/p38 ratio (normalized protein levels of app. 0.5 and 0.3, respectively) compared to the parental cell line RPE1 (normalized protein levels of 1.0), whereas RPT1 shows normalized protein levels of about 1.5.

To sum up, the ratio of pThr180/Tyr182-p38/p38 was decreased for HPT1, RPT3 and RPT4.

5 Discussion

5.1 Post-tetraploids derived from a non-transformed cell line are aneuploid and chromosomally unstable

The majority of newly formed tetraploid cells undergo highly erroneous mitosis resulting in chromosome missegregation and subsequent aneuploidy. Not only numerical aneuploidy, but structural chromosomal rearrangements can be facilitated by tetraploidy, as well (Fujiwara et al., 2005). Post-tetraploids derived from the transformed cell line HCT116, so called HPTs, proved to be aneuploid as well (Kuznetsova (2013); Fig. 5 C, D). Additionally, strong variations between early and late (36) passages were observed in the FISH experiment along with increased frequencies of mitotic errors (Kuznetsova (2013); Fig. 3 A) supporting the claim that a single passage through tetraploidy is sufficient to trigger a CIN phenotype. This finding was further confirmed for post-tetraploid cells that were derived from the non-transformed cell line RPE1, namely RPTs. Aneuploidy in two post-tetraploid cell lines, RPT1 and RPT3, was confirmed using FISH on chromosomes 3 and 7. Both cell lines displayed a bias towards chromosomal loss. Ongoing changes in chromosome copy numbers could however not be observed, most likely due to short passaging time (Fig. 4 B, C). Interestingly, most of the cells of RPT1 contained the expected chromosome number of four. About 20% of cells had three copies of chromosomes 3 and 7 in the FISH experiment. This suggests that RPT1 is an aneuploid cell line but the degree of aneuploidy is rather low. Alternatively, the gains and losses of chromosomes could be balanced within the cell population, which in turn would not change overall chromosome number distribution (e.g., if a certain number of cells with four chromosomes loses one chromosome, while the same number of cells with three chromosomes gain one chromosome, this change could be detected by neither FISH nor copy number variation analysis).

Compared to RPT1, the RPT3 cell line possessed three instead of four copies of chromosome 7 in the majority of analyzed cells, which is an indicator that the aneuploidy in RPT3 is more complex (Fig. 4 B, C). This is further supported by data from the copy number analysis by SNParrays. The analysis showed that RPT3 had lost one copy of many different chromosomes and additionally the copy number variations, which were present in the parental cell line are no longer maintained (Fig. 5 B). This indicates that RPT3 is a complex aneuploid cell line. Remarkably, previous reports on tetraploid derivatives from non-transformed cells, for example from p53-proficient mouse mammary epithelial cells (MMEC), state that those cells were not able to proliferate in culture. These deviations from my observations could be explained by the

fact that in the paper from Fujiwara et al. (2005) murine cells, but not human cells, were used. A second paper states that tetraploid cells could proliferate after tetraploidization but a part of the population was found to be chromosomally stable (Vitale et al., 2010). However, in this case tetraploidization was achieved by treatment with the microtubule poison nocodazole, resulting in mitotic slippage instead of inhibition of cytokinesis that was used by A. Kuznetsova for the generation of PTs. It is possible that the nocodazole treatment might, due to unknown reasons, affect the proliferation of tetraploid cells. Moreover, tetraploid cells generated by inhibition of cytokinesis and subsequent FACS sorting proved to be chromosomally stable (Ganem et al., 2009). It may be possible that the extent of aneuploidy does vary between post-tetraploid cell lines. RPT1 is more similar to the tetraploid derivatives observed in Ganem et al. (2009) than to RPT3. In contrast to that, RPT3 does show a high degree of aneuploidy following tetraploidization. Tetraploidy as a transient route to aneuploidy was already observed in HPTs (Kuznetsova, 2013) and was previously observed in other experimental settings, as well (Sansegret et al., 2011; Högnäs et al., 2012; Lv et al., 2012).

Remarkably, both HPT1 and RPT3 have lost one copy of chromosome 7. Loss of chromosome 7 or translocations of chromosome 7 are very often observed in leukemia and many lymphomas, which is a type of cancer where cells of the immune system are affected (Hasle et al., 1999; Russo et al., 1988; Brynes et al., 1996; Le Beau et al., 1986). These abnormalities also occur in some patients with aplastic anemia (Luna-Fineman et al., 1995). The aneuploidy of chromosome 7 is additionally linked to prostate cancer and is recognized as a marker of poor prognosis (Alcaraz et al., 1994). Furthermore, trisomy 7 is detected in more than 40% of colorectal adenomas. This abnormality is associated with growth advantage of cancer cells over normal diploid cells in serum-free conditions and is therefore considered to be a driving force in disease progression (Ly et al., 2011). An additional feature that PTs share with cancer cells is the bias towards chromosome loss (Duijf et al., 2013), which was observed in all analyzed post-tetraploids. Thus, post-tetraploid cells share features with known cancers such as the loss of chromosome 7, predominant loss rather than gain of chromosome copies and variable karyotypes (Storchova and Kuffer, 2008; Kuznetsova, 2013). In this light, to test the transformation potential of PT cell lines using *in vitro* colony formation assays, is an attractive venue for further research. To sum up, both cell lines derived from the non-transformed parental cell line RPE1 are aneuploid. However, the degree of aneuploidy varies more between the RPE1-derived post-tetraploids than between HCT116-derived post-tetraploids and the degree of aneuploidy positively correlates with the frequency of mitotic errors. (Fig 3 A). This might suggest that post-tetraploid cell lines derived from immortalized cells possess better genome stability surveillance

systems in comparison to those of post-tetraploid cell lines derived from transformed cells. Further research is required to address this possibility.

5.2 Nuclear p53 enrichment is attenuated after micronucleation in post-tetraploid cells

In Kuznetsova (2013), clones derived from HCT116 displayed increased frequencies of mitotic errors and were able to proliferate in a CIN state instead of arresting in a p53-dependent manner (Kuznetsova (2013); Fig. 3 C). However, the mechanisms underlying this tolerance are poorly understood. The p53 pathway is activated in response to many cellular stresses and targets damaged cells for cell arrest and apoptosis (Moll and Petrenko, 2003). One of the possible cellular stresses is missegregation that activates the p53 pathway as was observed in newly formed tetraploids (Kuffer et al., 2013). and in *de novo* aneuploids (Thompson and Compton, 2010). That prompted us to test the p53 response in PTs. A deregulation of the p53 pathway was confirmed by analysis of p53 enrichment after micronucleation, where HPTs enriched p53 in the nucleus less frequently than HCT116 in a micronucleation assay (Kuznetsova, 2013). In turn, from all RPE1-derived PTs, only RPT3 showed attenuated nuclear p53 enrichment in a micronucleation assay similar to HPTs (Fig. 6). This could suggest that only post-tetraploid cell lines with increased frequencies of missegregation are subjected to evolutionary pressure to become tolerant to missegregation. This tolerance may be achieved by attenuation of the nuclear p53 enrichment in response to missegregation.

Previously, the fact that the arrest or death in diploid cells and newly formed tetraploid cells following missegregation is dependent on p53 was observed in multiple experimental settings (Andreassen et al., 2001; Thompson and Compton, 2010) (for review: Vitale et al. (2011)). Furthermore, using transcriptional analysis it was shown that the p53 pathway was deregulated in HPT clones (Kuznetsova, 2013). On top of a deregulation of the p53 pathway on mRNA level, the possibility remains that p53 is mutated in missegregating PTs. Mutations of p53 are observed in the majority of sporadic human cancers (Brosh and Rotter, 2009). A mutation in the gene of the transcription factor p53 could affect its activation and stabilization by preventing e.g. necessary post-translational modifications. Additionally, mutations on TP53 deregulate a plethora of p53 target genes. These genes regulate very important cellular processes, such as cell cycle arrest, senescence, apoptosis, differentiation and DNA repair (for review: Moll and Petrenko (2003); Bullock and Fersht (2001); Brosh and Rotter (2009)). Therefore it is important to address the possibility of a mutation in TP53 by sequencing the PTs and their

parental cell lines.

Taken together, our findings support the hypothesis that post-tetraploids that display increased frequencies of missegregation become tolerant to missegregation by interfering with the p53 pathway.

5.3 Mechanisms that can contribute to tolerance to mitotic errors in PTs

All missegregating PTs displayed an attenuated nuclear p53 enrichment in a micronucleation assay (Fig. 6). It was previously shown in our laboratory that microtubule dynamics are slower at the microtubule plus-end during mitosis in HPTs compared to their parental cell line HCT116 (Fig. S4, Anastasia Kuznetsova, unpublished data). If minus-end dynamics are impaired similarly or to a higher degree as the respective dynamics at the plus-ends, it could potentially lead to a defect in p53 nuclear transport. In healthy cells, p53 gets transported to the nucleus by dynein when cells are experiencing increased cellular stress signals. Dynein moves along microtubules from the microtubule plus-ends to minus-ends, or in other words from the exterior into close proximity of the nucleus (Giannakakou et al., 2000; Schnapp and Reese, 1989; Hirokawa, 1998; Burakov and Nadezhdina, 2013; Moll et al., 1996). Disrupted microtubule dynamics could in turn disrupt the movement of dynein along microtubules, which may cause less p53 reaching the nucleus. Decreased nuclear p53 may result in a disruption of the p53 signaling pathway and may explain why HPTs do arrest or die less frequently after missegregation. This hypothesis needs testing on at least two levels. Firstly, do HPTs and RPT3 show disrupted microtubule dynamics at the minus-ends in a degree that would prevent/hinder the movement of dynein? Secondly, may the binding of p53 to dynein be impaired? This could be tested in interphase cells stained for dynein and p53. A closer look on the colocalization of p53 and dynein is necessary to evaluate this hypothesis.

An alternative hypothesis why PTs could be more tolerant to missegregation could be that missegregation does not lead to a proper p53 activation because the activation of p53 itself is impaired in PTs, which could prevent cells from arresting or dying. The activation of p53 is mediated by phosphorylation of serine 15 among others. The phosphorylated form of p53 can no longer interact with Mdm2, the negative regulator of p53 and therefore prevents its degradation by the proteasome (Shieh et al., 1997). This is supported by the fact that missegregation leads to increased p53 levels in HCT116 and RPE1, which are the parental cell lines used for

the generation of PTs (Thompson and Compton, 2010; Kuznetsova, 2013).

To investigate whether missegregation leads to defects in p53 activation, I performed immunoblotting against p53 and pSer15-p53 upon induced missegregation in a Vs83-washout experiment. Vs83 prevents the duplicated centrosomes from moving to the cell poles during mitosis, leading to erroneous microtubule-kinetochore attachments which often persist even after the drug is washed out. I assessed whether induced missegregation would lead to a decrease in the ratio of pSer15-p53/p53.

I found that none of the PTs showed a decreased ratio compared to their parental cell lines. Therefore it is unlikely that any link exists between chromosome missegregation, at least in Vs83-induced missegregation, and defects in p53 signaling identified by this experimental strategy (Fig. 7 C-F). There are two possible explanations for this result. Either there is no correlation between missegregation and a deregulated p53 pathway in PTs or, alternatively, immunoblotting as a population based approach is not the right choice to address this question. The latter is supported by the fact that a Vs83-washout does not only induce normal "mild" missegregation phenotypes but "severe" missegregation phenotypes, as well (Fig. 7 A, B). "Severe" missegregation can result in situations where about one third of the entire DNA mass is missegregated, which resembles tripolar mitosis. According to previous results, multipolar mitosis cannot be tolerated by HPTs (Fig. 3 D), suggesting that HPTs cannot tolerate such a massive DNA missegregation. The influence of "severe" missegregation on the westernblot is unknown. Therefore it would be necessary to consider testing this in another experimental setup. This could be addressed in a live-cell imaging approach. In live-cell imaging of all PTs and their respective parental cell lines as a control it would be possible to assess the missegregation phenotypes. In fixing the cells immediately after finishing live-cell imaging and immunostaining against p53 and pSer15-p53, the p53 activation could be assessed only in cells that showed the desired phenotype of "mild" missegregation.

Taken together, one possible pathway for PTs to become tolerant to chromosome missegregation is an attenuation of nuclear p53 enrichment following missegregation. This may be achieved due to impaired nuclear import of p53. A link between induced missegregation and impaired p53 activation could however not be shown in an immunoblotting approach. At this stage the mechanism of tolerance to missegregation in PTs is still elusive.

5.4 Response to DNA damage is altered in PTs

Since there was no correlation observed between induced missegregation via a Vs83-washout and deregulation of the p53 activation in post-tetraploids (Fig. 7 D, F), I tested if other cellular stress signals that are linked to missegregation could impair p53 activation. It was proposed that missegregation induces DNA double strand breaks either by forces generated during cytokinesis or by the mitotic spindle (Janssen et al., 2011; Guerrero et al., 2010). Thus, under the assumption that missegregation in PTs is further causing DNA damage, potential alteration in the DNA damage response might at least contribute to tolerance to missegregation. To test this possibility, I induced DNA damage with doxorubicine (DRB). Treatment with DRB leads to single- and double strand breaks (Tewey et al., 1984).

Phosphorylation of p53 was observed to be impaired in the immunoblotting experiments for HPT2, HPT4 and all RPTs (Fig. 8 B, E). For HPT2 and RPT4, the decrease in the ratio of pSer15-p53/p53 was statistically significant. This indicates that the activation of p53 is impaired in response to DNA damage. Additionally, it does not seem to matter from which parental cell line the post-tetraploids are derived, since all HPTs with the exception of HPT1 and all RPTs showed decreased activation of p53.

Serine 15 of p53 is phosphorylated by many different kinases, such as p38, ATM and ATR (Banin, 1998; Tibbetts et al., 1999; Bulavin et al., 1999; Vitale et al., 2008; She et al., 2000). Activated p38 phosphorylates p53 on serine 15 directly after induced DNA damage (Vitale et al., 2008; She et al., 2000; Bulavin et al., 1999). Furthermore, p38 is involved in the response to missegregation (Thompson and Compton, 2010) and plays a role in G1-S arrest in response to centrosome defects (Mikule et al., 2006). I analyzed whether activation of the stress kinase p38 is impaired by performing immunoblotting experiments against p38 and pThr180/Tyr182-p38. p38 is activated by a dual phosphorylation of threonine 180 and tyrosine 182 in response to cellular stress signals and pro-inflammatory cytokines (Raingeaud et al., 1995). HPT1, RPT3 and RPT4 showed an impaired activation of p38 in response to DNA damage. An impairment of p38 signaling coincides with the appearance of longer spindles (Lee et al., 2010). This can also be observed in HPT1 and HPT2 (Fig. S3, Kuznetsova (2013)) which have significantly longer spindles compared to their parental cell line HCT116. This supports the findings that p38 signaling is altered in some of the post-tetraploids. Furthermore, these cell lines also have an increased spindle width and a resulting larger spindle angle (Fig. S3, Kuznetsova (2013)). Taken together, these findings suggest that DNA damage is sensed less efficiently on two members of the p53 pathway: p53 itself and one of its upstream activators p38. Whether only the

activation of p38 is impaired in PTs, which in turn impairs activation of p53 or whether the activation of both p38 and p53 are independently altered cannot be distinguished using the data currently available. A possible way to examine if the p53 activation is impaired independently of the impairment of p38 would be a p38 knockdown and subsequent immunoblotting against p53 and pSer15-p53. If the p53 activation is impaired in cells lacking p38, the impairment of p53 is independent of p38. Assuming that missegregation does indeed lead to DNA damage in PTs, tolerance to missegregation may be explained by these results under the assumption that the Vs83-washout data are flawed or that missegregation induced by a Vs83-washout differs from naturally occurring missegregation, at least when it comes to the cells' response.

Freshly arising tetraploids arrest in an ATM dependent manner (Kuffer et al., 2013). Therefore it would be interesting to investigate whether the proliferation of PTs despite increased frequencies of mitotic errors could be caused by impaired ATM signaling. ATM is activated upon chromosome missegregation which leads to DNA double strand breaks since they are subjected to forces during cytokinesis (Janssen et al., 2011; Li et al., 2010). ATM and its homologue ATR are essential to modulate cell progression, DNA repair and apoptosis. ATM is required for the phosphorylation of several cell-cycle regulators, e.g. p53, Mdm2, Chk2 (Bakkenist and Kastan, 2004; Shiloh, 2003; Abraham, 2001). It phosphorylates p53 on serine 15 directly upon DNA damage (Banin, 1998; Canman et al., 1998). It would be interesting to test whether the activity of ATM is impaired in PTs as well in order to gain insight what causes the impairment of p53 activation. The abundance of ATM and activated, phosphorylated ATM could be tested in an immunoblotting experiment in DRB-treated and untreated cells to show whether ATM activation upon DNA damage is impaired which would in turn lessen the ability of ATM to activate p53.

In summary, the activation of p53 and at least one of its upstream regulators, p38, in response to DNA damage seems to be impaired in post-tetraploids. Post-tetraploids might therefore be tolerant to missegregation because missegregation induced DNA damage is sensed less efficiently by the p53 pathway.

5.5 Oxidative DNA damage could be sensed less efficiently in PTs

Missegregation is linked to DNA damage in the form of double strand breaks (Janssen et al., 2011; Guerrero et al., 2010) as well as to oxidative DNA damage (Li et al., 2010). Both types of DNA damage activate ATM (Li et al., 2010; Guo et al., 2010; Janssen et al., 2011). In addition, a correlation between missegregation and oxidative DNA damage was found in freshly formed

tetraploids. It has been shown that they exhibit increased levels of oxidative DNA damage, measured by the accumulation of 8-hydroxy-2-deoxyguanosine (8-OHdG), a marker for oxidative DNA damage. These increased levels of oxidative DNA damage correlated with increased nuclear p53 levels upon missegregation in newly formed tetraploids (Kuffer et al., 2013). The question arises whether PTs might be tolerant to missegregation by increasing their tolerance to canonical and/or oxidative DNA damage. It is however not possible to distinguish these two types of DNA damage with the data from this study, because DRB does not only induce single and double strand breaks but was shown to induce oxidative stress in cardiac myocytes in rats (Zhou et al., 2001). The aforementioned suggested experiments regarding the levels of unactivated and activated ATM in the presence of DNA damage in PTs would only show whether the ATM activation is impaired in general. If this were found to be the case, the experiment should be refined by changing the DNA damaging reagent to be able to separate canonical and oxidative damage. Another point is that p38 is activated upon oxidative stress (Gutiérrez-Uzquiza et al., 2012). Therefore, the same points as for the proposed ATM experiments hold true for p38, as well.

In the future, a first prerequisite would be to test whether PTs display an increase in oxidative and/or canonical DNA damage upon missegregation. If missegregation in PTs causes oxidative and/or canonical DNA damage, a possible way to distinguish the PTs' reaction to oxidative as opposed to canonical damage would be to repeat the above described experiments, but with a reagent that induces oxidative DNA damage only, e.g. menadione.

To sum up all the previous discussion, a key hallmark of PTs seems to be aneuploidy independent of the type of their parental cell lines. However, the degree of aneuploidy varied and not all cells derived from an immortalized parental cell line displayed complex aneuploidy. CIN, which was found in all PTs derived from a cancerous cell line could not be clearly identified to be present in all RPTs. This fact needs to be addressed by increasing the number of passages before looking at their chromosomal copy numbers. Post-tetraploids seem to share features with known cancers, such as the loss of chromosome 7, more frequent chromosome losses than gains and karyotypic variability.

Nonetheless, this study suggests a possible reason for tolerance to missegregation in PTs. It could be that missegregation leads to oxidative and/or canonical DNA damage, while the response to this damage is impaired by unknown factors. The key element in response to these damages seems to be the p53 pathway with p53 itself building the possible bottleneck of the pathway. This means that if p53 activation is impaired, as was shown, the consecutive

answer/response such as apoptosis or cell arrest caused by p53 may be diminished. Several possible candidates can activate p53 and their role in tolerance to missegregation needs to be further analyzed.

6 Materials and Methods

6.1 Cell lines

Tab. 1: Used cell lines and descriptions

Cell line	Origin	Source
HCT 116 H2B-GFP	human colorectal carcinoma cell line	ATCC (No. CCL- 247, LGC Standards GMBH, Wesel, Germany; H2B-GFP expression established by Christian Kuffer)
HPT1 H2B-GFP	posttetraploid derivative of HCT 116 H2B-GFP	established by Dr. Anastasia Y. Kuznetsova
HPT2 H2B-GFP	posttetraploid derivative of HCT 116 H2B-GFP	established by Dr. Anastasia Y. Kuznetsova
HPT4 H2B-GFP	posttetraploid derivative of HCT 116 H2B-GFP	established by Dr. Anastasia Y. Kuznetsova
RPE 1 hTERT H2B-GFP	human retinal pigment epithelium cell line, immortalized by telomerase expression	Dr. Stephen Taylor
RPT1 H2B-GFP	posttetraploid derivative of RPE1 hTERT H2B-GFP	established by Dr. Anastasia Y. Kuznetsova
RPT3 H2B-GFP	posttetraploid derivative of RPE1 hTERT H2B-GFP	established by Dr. Anastasia Y. Kuznetsova
RPT4 H2B-GFP	posttetraploid derivative of RPE1 hTERT H2B-GFP	established by Dr. Anastasia Y. Kuznetsova

All post-tetraploid derivatives were generated by treatment with dihydrocytochalasin D (DCD, 0.75 μM) that inhibits cytokinesis. Cells were subcloned after DCD washout by limited dilution on 96-well plates (seeding of dilution: 0.5 cells per well). DNA content was assessed using flow cytometry for individual clones. Clones with a near-tetraploid DNA content were termed post-tetraploid derivatives and used in this work.

6.2 Primary antibodies

Tab. 2: Used primary antibodies and descriptions

Antibody	Species	Dilution	Source	Catalogue number
p53	rabbit	1:100	Cell Signalling	#9286
Mdm2	mouse	1.140	abcam	ab16895
p21	rabbit	1:800	Cell Signalling	#2947
phospho-p38 (Thr180, Tyr182)	rabbit	1:800	Cell Signalling	#9211
p38	rabbit	1:700	Cell Signalling	#9212
phospho-p53 (Ser15)	rabbit	1:200	Cell Signalling	#9284
phospho-p53 (Ser15)	mouse	1:1000	Cell Signalling	#9286
GAPDH	rabbit	1:1000-1:5000	Cell Signalling	#2118
HSP90	rabbit	1:2500-1:5000	Cell Signalling	#4874

All antibodies were diluted in the appropriate blocking solution (5% of BSA or skim milk in TBS-T).

6.3 Materials and solutions

6.3.1 SDS-PAGE and immunoblotting materials

Gels: 10% resolving polyacrylamide gels with 5% stacking gels.

RIPA lysis buffer (pH 7.5): 50 mM HEPES, 150 mM NaCl, 1.5 mM MgCl₂, 1 mM EGTA, 10% glycerol, 1% TritonX-100, 100 mM NaF, 10 mM *Na*₄*P*₂*O*₇, protease inhibitor cocktail.

Lämmli buffer: 62.5 mM Tris/HCl pH 6.8, 2% (w/v) glycerol, 0.002% (w/v) bromphenole blue, 2.5% β-mercaptoethanol.

Lower SDS-buffer (pH 8.8): 1.5 M Tris-HCl, 0.4% (w/v) SDS.

Upper SDS-buffer (pH 6.8): 0.5 M Tris-HCl, 0.4% (w/v) SDS.

SDS-PAGE running buffer: 25 mM Tris/HCl, 200 mM glycine, 0.1% (w/v) SDS.

Semi-dry transfer buffer: 27 mM Tris/HCl, 200 mM glycine, 20% (w/v) methanol (absolute).

TBS-T (pH 7.5): 50 mM Tris, 150 mM NaCl.

Blocking buffer: 5% (w/v) skim milk or BSA in TBS-T.

6.3.2 Other materials

PBS (pH 7.5): 137 mM NaCl, 2.7 mM KCl, 10 mM Na_4HPO_4 , 2 mM KH_2PO_4 . All other materials used are described in the method section.

6.4 Cell culture

6.4.1 Working cell stocks

Working stocks in vials were preserved in a freezing solution (90% fetal calf serum FCS, 10% DMSO) and stored at -80°C in a freezer. To thaw the cells, the vials were agitated at 37°C in a water bath. Cells were transferred to falcon tubes containing 5 mL of medium. Cells were pelleted at 1500 rpm for 5-7 minutes. Supernatant was removed and cells were resuspended in 10 mL of fresh medium and plated in 10 cm Petri dishes.

6.4.2 Culturing

All cell lines were cultured in Dulbecco's modified medium (DMEM, Gibco, Karlsruhe, Germany) with 10% heat-inactivated FCS (55°C, 45-60 min) and 1-2% PenStrep (50 IU/mL penicillin and 50 $\mu g/mL$ streptomycin, PAA, Pasching, Austria) at 37°C and 5% CO_2 in a humid atmosphere. Cell cultures were used for experiments after 2 to 4 days in culture.

Cells were split three times a week, in a ratio from 1:2 to 1:10 depending on density and planned experiments. Cells were washed in PBS, treated with a small amount of trypsin-EDTA (PAA, Pasching, Austria) covering the plate completely for 3-5 minutes at 37°C until they detached completely. The appropriate amount was plated in new Petri dishes, keeping the amount of trypsin-EDTA well below 25%. Cells were counted on a Beckman Coulter Z1 cell counter (Beckman Coulter, Munich, Germany) prior to seeding for experiments. Cells were diluted in medium to obtain the needed concentrations.

For Western blots, 10 mL of cell solution with a concentration of 170000 cells/mL were plated in a 10 cm Petri dish for all cell lines. For live-cell imaging ,170000 cells/mL were dispensed in 100 μL steps in a 96-well plate (black well glass bottom plates, Greiner bio-one, Kremsmünster, Austria).

6.5 MycoTrace

All cell lines were tested for mycoplasm infection with the MycoTrace kit from PAA. Cell culture supernatant (approximately 1-2 mL/ cell line) was collected and 1 mL was transferred into Eppendorf tubes. The supernatant was centrifuged for 5 minutes at 13000 rcf. The supernatant was removed by decanting and careful pipetting. The pellet was resuspended in 100 μ L DNase free water and heated at 95°C in a heatblock for 3 minutes. The samples were centrifuged for 5 minutes at 13000 rcf and the supernatent was transferred to a new tube. A mastermix was prepared for all samples, the water control (no sample, no internal control), the internal control (no sample) and the positive control (positive tested sample, personal communication Christian Kuffer).

Tab. 3: Preparation of the PCR reaction mixture for MycoTrace samples

Components	Volumes needed [μ L]
Taq Polymerase Buffer	2.7
MycoTrace Primer Mix	9.0
Myco Trace Internal control	1.0
Sample	1.0
Water	9.3
Taq Polymerase (1 U/mL)	1.0

PCR condition: 94/60"- [94/30"-61/30"-72/30"]x35-72/10'

The samples were mixed with 6x loading dye and loaded in a 2% gel. The gel run was 30 minutes at 100 V and then 30 minutes at 135 V. The image was visualized under UV light.

6.6 Used drugs to assess p53 response

Cells were treated with 1 μ M DRB, which induces severe DNA damage for 4 hours, pelleted and either flash-frozen in liquid nitrogen and stored at -80°C or lysed immediately. The response was compared to untreated, diploid cells as a negative control and freshly tetraploid cells, which were obtained by treatment with DCD (dihydrocytochalasin D, 0.75 μ M, Sigma, Taufkirchen, Germany), an actin inhibitor which abolishes cytokinesis, for 24 hours. Cells were treated with 20 μ M Vs83 (a kinesin inhibitor) for 18 hours. Cells were washed 6-7 times with PBS and released in prewarmed medium. The cells were monitored and pelleted approximately 6-7 hours after they left mitosis.

6.7 Cell lysis, protein preparation and concentration measurement

Pelleted cells were resuspended in 100-400 μL RIPA lysis buffer containing protease inhibitor cocktail (Pefabloc SC, Roth, Karlsruhe, Germany). Lysates in Eppendorf tubes were incubated on ice for 10 minutes, then sonicated in a waterbath for 15 minutes. Cell debris was pelleted by centrifugation at 13600 rpm for 10 minutes at 4°C using a table-top microcentrifuge (Eppendorf, Hamburg, Germany). Supernatant was transferred to a new, precooled tube. Protein concentration was measured at 595 nm wavelength in triplicates or quadruplicates using Bradford reagent on SmartSpec 3000 spectrophotometer (both, BioRad, Munich, Germany). The median of the measurements was used for further calculations. Protein levels were adjusted to concentration of 15 to 30 $\mu g/\mu L$ using the appropriate amount of 4x Lämmlli-buffer.

6.8 SDS-PAGE and immunoblotting

Cell lysates (20 μL per pocket) were loaded into an SDS-gel and separated (90 V, 90 mA, appr. 1:30 h). Protein sizes were estimated using PrecisionPlus All Blue protein markers (BioRad, Munich, Germany; 10 μL per pocket). Separated proteins were transferred semi-dry (10 V, 300 A, 40 min; Trans-Blot Semi Dry BioRad, Munich, Germany) onto a water-activated Whatman Protran nitrocellulose membrane (Sigma-Aldrich, St. Louis, MO, USA). Proteins on membranes were visualized by ponceau S staining (0.2% ponceau S, 1% acetic acid). Membranes were blocked for 3 hours in blocking solution and were further incubated in primary antibody solutions (Tab. 2) or in blocking solution (primary antibodies next day for 1 h) overnight at 4°C on a rotor. Membranes were rinsed three times for 5 minutes each with TBS-T, incubated for one hour in HRP-conjugated secondary antibodies (R&D Systems) in blocking solution (dilution 1:5000). Membranes were rinsed three times for 5 minutes each with TBS-T, and incubated for 5 minutes in Super Signal West Femto Maximum Sensitivity Substrate (Thermo Scientific), ECL Prime Western Blotting Detection Reagent (GE Healthcare), or TMA-6 kit (Lumigen) and detected on Fujifilm Luminescent Image Analyzer (LAS-3000 Lite) system (Fujifilm, Düsseldorf, Germany) and ECL hyperfilm (GE Healthcare).

Quantification of desired protein bands was done with the help of ImageJ (National Institutes of Health, <http://rsb.info.nih.gov/ij/>). Bands were normalized over the GAPDH or HSP90 band or ponceau staining and further normalized to diploid control. Graphs were designed in prism (GraphPad Software, San Diego California USA, www.graphpad.com)

6.9 Micronucleation test

Cells were seeded on a glass-bottom 96-well plate two days before imaging. To mark cells which underwent mitosis, all cells were treated with DCD for 18 hours. Cells that underwent one single mitosis before fixation become binucleated and were scored.

Cells were washed three time with PBS, fixed by adding 100 μL 37% formaldehyde directly into the medium. Incubation for 12 minutes. Cells were thrice rinsed with PBS and treated with PBS containing 0.5% TritonX100 (Roth, Karlsruhe, Germany) for 5 minutes to permeabilize. Cells were washed three times with PBS and blocked for 30 minutes in 5% FCS with 0.3% TritonX100. Cells were incubated in rabbit anti-p53 antibody (1:600, Cell Signalling #9286) in blocking solution in the fridge over night.

Cells were washed three times with PBS and were incubated for one hour in secondary antibody solution (1:1000, DyLight 649-conjugated anti-rabbit, Thermo Fisher Scientific Inc.) and stained with SYTOX Green Nucleic Acid dye (Molecular Probes, Invitrogen) with added RNase. Cells were washed four times with PBS and imaged in the last volume of PBS. Acquisition on an inverted Zeiss Observer Z1 microscope with 20x magnification air objective with Slidebook 5.5 software. The brightness of the p53 staining in the nucleus and cytoplasm was determined with Cell Profiler software. The percentage of binucleated cells containing a micronucleus was determined. The p53 enrichment in the nucleus was correlated to cell fate.

6.10 Analysis of mitotic abnormalities

The cells were seeded on a glass-bottomed 96-well plate. Cells were briefly washed with PBS, fixed with 100% methanol for 10 minutes at -20°C. Cells were thrice rinsed with PBS. DNA was stained with SYTOX Green Nucleic Acid dye (Molecular Probes, Invitrogen) with added RNase. The acquisition was carried out on Visitron Systems microscope using GFP and DIC filters and 20x magnification objective with Slidebook 5.5 software. The lagging DNA mass and anaphase bridges were scored in anaphases and early telophases by visual inspection of the images.

6.11 Interphase FISH

The cell lines RPE1, RPT1 and RPT3 were seeded at 0 and 12 passages in 10 cm plates. Cells were treated for 4.5 hours with 50 $ng/\mu L$ colchicine (Serva, Heidelberg, Germany) to depolymerize microtubules in order to obtain a higher number of cells in mitosis. Cells were collected and pelleted with a table-top centrifuge at 1500 rpm for 4 minutes. Cells were swollen in 6 mL

per falcon tube of 75 mM KCl (Roth, Karlsruhe, Germany) for 15 minutes at 37°C. Cells were fixed in 6 mL per falcon tube ice-cold Carnoy solution (75% absolute methanol, 25% acetic acid, Sigma, Taufkirchen, Germany). The fixative was exchanged three times by spinning the tubes at 800 rpm for 6 minutes, supernatant was removed and cells were carefully resuspended in fixative. The last volume was adjusted in a way that all cells should have the same density and stored over night at 4°C.

Per cell line, 15 μ L of cell suspension was spotted on a glass microscope slide and the drop was allowed to dry. The cell density was checked and adjusted when needed. Dry slides were immersed in 2x SSC for 2 minutes at room temperature without agitation. The slides were dehydrated in an ethanol series (70%, 85%, 100% absolute ethanol) for two minutes each step at room temperature without agitation.

The probe (α -satellite at chromosome 3 with a red fluorophore (LPE003R) and α -satellite at chromosome 7 with a green fluorophore (LPE007G), Cytocell aquarius, Cambridge, UK) was thawed at room temperature. 3 μ L of each probe and 4 μ L per slide were mixed in an aluminum-foil covered Eppendorf tube by vortexing and pulse-spun in a table-top centrifuge.

The probe and the slides were prewarmed at 37°C for 5 minutes. 10 μ L of probe mixture were spotted onto the cell sample. A coverslip was applied and sealed with rubber solution glue (Fixogum, Marabu). When the glue was completely dry, the samples were denaturated on a hotplate at 75°C for 2 minutes. The slides were placed in a humid, lightproof container. The container was sealed with parafilm and placed at 37°C over night for hybridization.

The coverslips and all remaining rubber glue were removed carefully. The slides were immersed without agitation in 0.25x SSC (pH 7.0) for 2 minutes at 72°C. The slides were drained and immersed without agitation in 2x SSC, 0.05% Tween-20 (pH 7.0) for 2 minutes at room temperature. Slides were drained and 10 μ L DAPI antifade was added onto each sample. The slides were covered with coverslips and sealed with rubber glue. DAPI on the slides was developed in the dark and glue was allowed to dry completely. The slides were acquired on an inverted Zeiss Observer Z1 microscope with 63x magnification oil objective with Slidebook 5.5 software. Per slide, captures of approximately 200 cells were taken. The number of chromosomes 3 and 7 per cell was determined visually.

6.12 Copy Number Analysis

In collaboration with Kloosterman, W.P., Uni Utrecht, NL.

Human CytoSNP-12 bead chip arrays (Illumina) for detecting copy number aberrations (CNAs)

were used in clonal aneuploid and diploid cell lines. Array hybridization was performed according to the manufacturer's recommendations. CNAs were called using Nexus software (version 7.5.1) with standard settings. To identify unique CNAs in clonal cell lines, we used the Nexus call coordinates and removed all calls of the same type with a reciprocal overlap of at least 60%. Unique CNA calls were manually curated based on copy number and allele frequency profiles.

7 Supplementaries

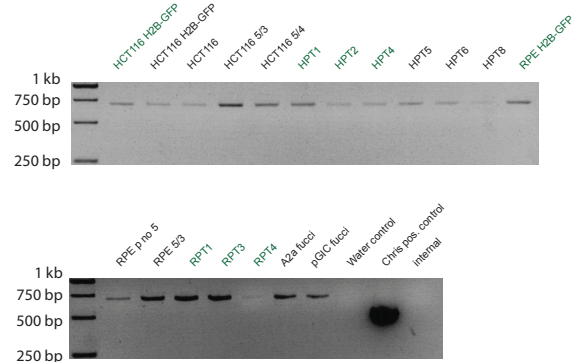


Fig. S1: Test for mycoplasm infection in all cell lines with the PAA MycoTrace kit. PCR based detection of various mycoplasm strains in the cell culture supernatant of cultured cells. PCR products were loaded into a 2% TAE-gel and separated. All PCR samples were pipetted with an internal control (700 bp). Mycoplasm infection would be visible by an 500 bp band. Green marked bands are from cell lines used in this work.

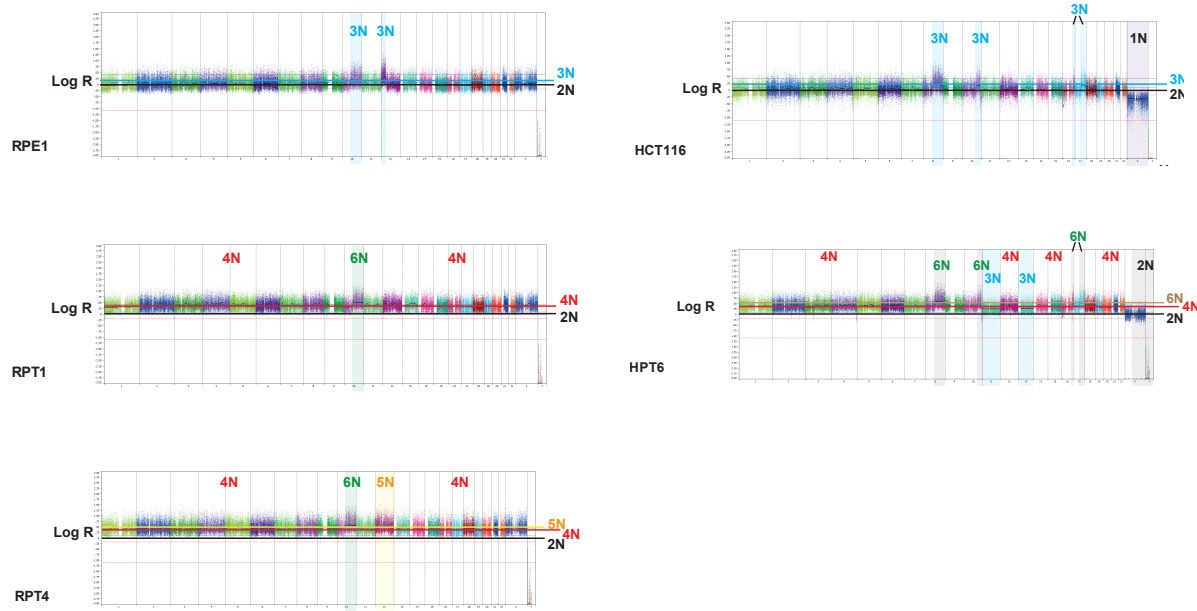


Fig. S2: Characterization of post-tetraploid cell lines derived from RPE1 and HCT116 by Copy Number Analysis. Copy number analysis data in collaboration with Kloosterman, W.P., Uni Utrecht, NL for RPE1, HCT116, RPT1, HPT6 and RPT4

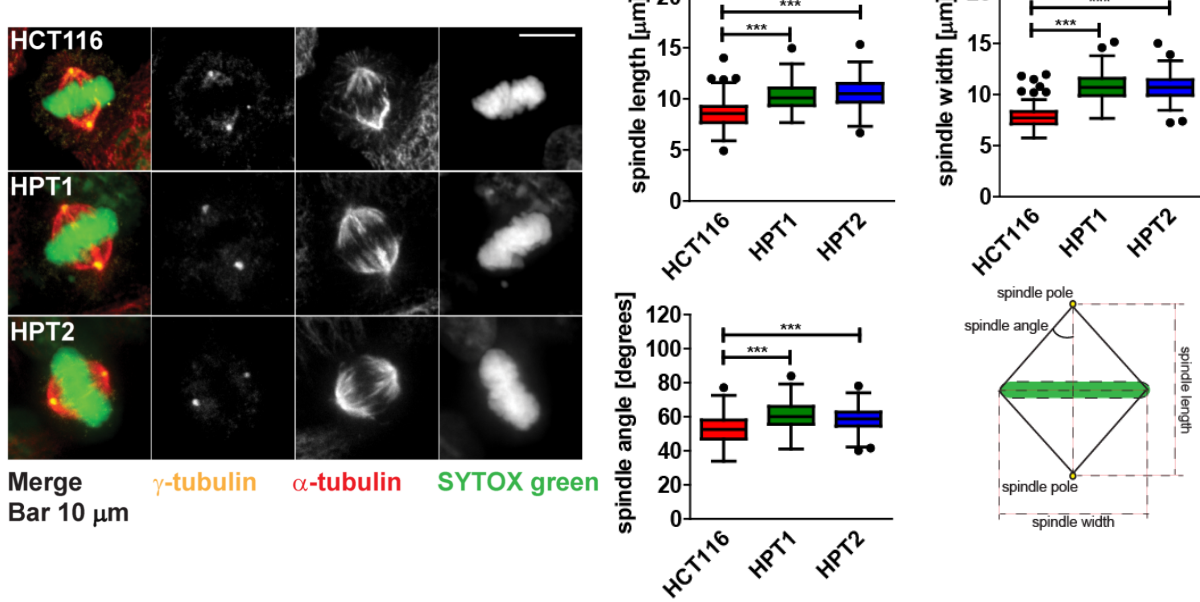


Fig. S3: **Mitotic spindle is altered in HPTs.** Spindle length and width is changed in HPTs. Data and Images from Anastasia Kuznetsova (Kuznetsova, 2013).

Significance levels: * denotes $p \leq 0.05$, ** denotes $p \leq 0.01$, *** denotes $p \leq 0.001$

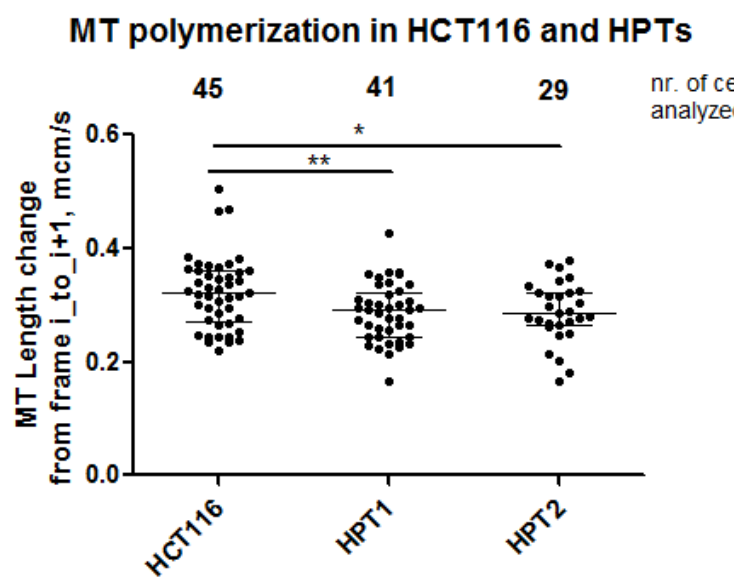


Fig. S4: **Changes in microtubule polymerization in HPTs.** Change of length in microtubule plus ends. 5-10 microtubules analyzed per cell in three independent experiments. Data and Images from Anastasia Kuznetsova, unpublished data.

Significance levels: * denotes $p \leq 0.05$, ** denotes $p \leq 0.01$, *** denotes $p \leq 0.001$

8 Literature

- Abraham, R. T. (2001). Cell cycle checkpoint signaling through the ATM and ATR kinases. *Genes & development*, 15(17):2177–96.
- Aguirre-Portolés, C., Bird, A. W., Hyman, A., Cañamero, M., Pérez de Castro, I., and Malumbres, M. (2012). Tpx2 controls spindle integrity, genome stability, and tumor development. *Cancer research*, 72(6):1518–28.
- Alcaraz, A., Takahashi, S., Brown, J. A., Herath, J. F., Bergstrahl, E. J., Larson-Keller, J. J., Lieber, M. M., and Jenkins, R. B. (1994). Aneuploidy and aneusomy of chromosome 7 detected by fluorescence in situ hybridization are markers of poor prognosis in prostate cancer. *Cancer research*, 54(15):3998–4002.
- Anderson, G. R., Stoler, D. L., and Brenner, B. M. (2001). Cancer: the evolved consequence of a destabilized genome. *BioEssays : news and reviews in molecular, cellular and developmental biology*, 23(11):1037–46.
- Andreassen, P. R., Lohez, O. D., Lacroix, B., and Margolis, R. L. (2001). Tetraploid State Induces p53-dependent Arrest of Nontransformed Mammalian Cells in G1. 12(May):1315–1328.
- Bakhoum, S. F. and Compton, D. A. (2012). Chromosomal instability and cancer: a complex relationship with therapeutic potential. *The Journal of clinical investigation*, 122(4):1138–43.
- Bakkenist, C. J. and Kastan, M. B. (2004). Initiating cellular stress responses. *Cell*, 118(1):9–17.
- Banin, S. (1998). Enhanced Phosphorylation of p53 by ATM in Response to DNA Damage. *Science*, 281(5383):1674–1677.
- Beroukhim, R., Mermel, C. H., Porter, D., Wei, G., Raychaudhuri, S., Donovan, J., Barretina, J., Boehm, J. S., Dobson, J., Urashima, M., Mc Henry, K. T., Pinchback, R. M., Ligon, A. H., Cho, Y.-J., Haery, L., Greulich, H., Reich, M., Winckler, W., Lawrence, M. S., Weir, B. A., Tanaka, K. E., Chiang, D. Y., Bass, A. J., Loo, A., Hoffman, C., Prensner, J., Liefeld, T., Gao, Q., Yecies, D., Signoretti, S., Maher, E., Kaye, F. J., Sasaki, H., Tepper, J. E., Fletcher, J. A., Tabernero, J., Baselga, J., Tsao, M.-S., Demichelis, F., Rubin, M. A., Janne, P. A., Daly, M. J., Nucera, C., Levine, R. L., Ebert, B. L., Gabriel, S., Rustgi, A. K.,

- Antonescu, C. R., Ladanyi, M., Letai, A., Garraway, L. A., Loda, M., Beer, D. G., True, L. D., Okamoto, A., Pomeroy, S. L., Singer, S., Golub, T. R., Lander, E. S., Getz, G., Sellers, W. R., and Meyerson, M. (2010). The landscape of somatic copy-number alteration across human cancers. *Nature*, 463(7283):899–905.
- Boveri, T. (2008). Concerning the Origin of Malignant Tumours by Theodor Boveri. Translated and annotated by Henry Harris. *Journal of Cell Science*, 121(Supplement 1):1–84.
- Brito, D. a. and Rieder, C. L. (2006). Mitotic checkpoint slippage in humans occurs via cyclin B destruction in the presence of an active checkpoint. *Current biology : CB*, 16(12):1194–200.
- Brosh, R. and Rotter, V. (2009). When mutants gain new powers: news from the mutant p53 field. *Nature reviews. Cancer*, 9(10):701–13.
- Brynes, R. K., Almaguer, P. D., Leathery, K. E., McCourt, A., Arber, D. A., Medeiros, L. J., and Nathwani, B. N. (1996). Numerical cytogenetic abnormalities of chromosomes 3, 7, and 12 in marginal zone B-cell lymphomas. *Modern pathology : an official journal of the United States and Canadian Academy of Pathology, Inc*, 9(10):995–1000.
- Bulavin, D. V., Saito, S., Hollander, M. C., Sakaguchi, K., Anderson, C. W., Appella, E., and Fornace, a. J. (1999). Phosphorylation of human p53 by p38 kinase coordinates N-terminal phosphorylation and apoptosis in response to UV radiation. *The EMBO journal*, 18(23):6845–54.
- Bullock, a. N. and Fersht, a. R. (2001). Rescuing the function of mutant p53. *Nature reviews. Cancer*, 1(1):68–76.
- Burakov, A. V. and Nadezhina, E. S. (2013). Association of nucleus and centrosome: magnet or velcro? *Cell biology international*, 37(2):95–104.
- Cahill, D. P., Lengauer, C., Yu, J., Riggins, G. J., Willson, J. K., Markowitz, S. D., Kinzler, K. W., and Vogelstein, B. (1998). Mutations of mitotic checkpoint genes in human cancers. *Nature*, 392(6673):300–3.
- Caldwell, C. M., Green, R. a., and Kaplan, K. B. (2007). APC mutations lead to cytokinetic failures in vitro and tetraploid genotypes in Min mice. *The Journal of cell biology*, 178(7):1109–20.

- Canman, C. E., Lim, D. S., Cimprich, K. A., Taya, Y., Tamai, K., Sakaguchi, K., Appella, E., Kastan, M. B., and Siliciano, J. D. (1998). Activation of the ATM kinase by ionizing radiation and phosphorylation of p53. *Science (New York, N.Y.)*, 281(5383):1677–9.
- Carter, S. L., Eklund, A. C., Kohane, I. S., Harris, L. N., and Szallasi, Z. (2006). A signature of chromosomal instability inferred from gene expression profiles predicts clinical outcome in multiple human cancers. *Nature genetics*, 38(9):1043–8.
- Cimini, D., Howell, B., Maddox, P., Khodjakov, a., Degrassi, F., and Salmon, E. D. (2001). Merotelic kinetochore orientation is a major mechanism of aneuploidy in mitotic mammalian tissue cells. *The Journal of cell biology*, 153(3):517–27.
- Connell, J. W., Lindon, C., Luzio, J. P., and Reid, E. (2009). Spastin couples microtubule severing to membrane traffic in completion of cytokinesis and secretion. *Traffic (Copenhagen, Denmark)*, 10(1):42–56.
- Cooke, M. S., Evans, M. D., Dizdaroglu, M., and Lunec, J. (2003). Oxidative DNA damage: mechanisms, mutation, and disease. *FASEB journal : official publication of the Federation of American Societies for Experimental Biology*, 17(10):1195–214.
- Crasta, K., Ganem, N. J., Dagher, R., Lantermann, A. B., Ivanova, E. V., Pan, Y., Nezi, L., Protopopov, A., Chowdhury, D., and Pellman, D. (2012). DNA breaks and chromosome pulverization from errors in mitosis. *Nature*, 482(7383):53–8.
- Deng, C., Zhang, P., Harper, J. W., Elledge, S. J., and Leder, P. (1995). Mice lacking p21CIP1/WAF1 undergo normal development, but are defective in G1 checkpoint control. *Cell*, 82(4):675–84.
- Dewhurst, S. M., McGranahan, N., Burrell, R. a., Rowan, A. J., Grönroos, E., Endesfelder, D., Joshi, T., Mouradov, D., Gibbs, P., Ward, R. L., Hawkins, N. J., Szallasi, Z., Sieber, O. M., and Swanton, C. (2014). Tolerance of whole-genome doubling propagates chromosomal instability and accelerates cancer genome evolution. *Cancer discovery*, 4(2):175–85.
- Doxsey, S., Zimmerman, W., and Mikule, K. (2005). Centrosome control of the cell cycle. *Trends in cell biology*, 15(6):303–11.
- Duelli, D. M., Padilla-Nash, H. M., Berman, D., Murphy, K. M., Ried, T., and Lazebnik, Y. (2007). A virus causes cancer by inducing massive chromosomal instability through cell fusion. *Current biology : CB*, 17(5):431–7.

Duesberg, P. and Li, R. (2003). Multistep carcinogenesis: a chain reaction of aneuploidizations. *Cell cycle (Georgetown, Tex.)*, 2(3):202–10.

Duesberg, P., Stindl, R., and Hehlmann, R. (2000). Explaining the high mutation rates of cancer cells to drug and multidrug resistance by chromosome reassortments that are catalyzed by aneuploidy. *Proceedings of the National Academy of Sciences of the United States of America*, 97(26):14295–300.

Duijf, P. H. G., Schultz, N., and Benezra, R. (2013). Cancer cells preferentially lose small chromosomes. *International journal of cancer. Journal international du cancer*, 132(10):2316–26.

Eiben, B., Bartels, I., Bähr-Porsch, S., Borgmann, S., Gatz, G., Gellert, G., Goebel, R., Hammans, W., Hentemann, M., and Osmers, R. (1990). Cytogenetic analysis of 750 spontaneous abortions with the direct-preparation method of chorionic villi and its implications for studying genetic causes of pregnancy wastage. *American journal of human genetics*, 47(4):656–63.

El-Deiry, W. S., Tokino, T., Velculescu, V. E., Levy, D. B., Parsons, R., Trent, J. M., Lin, D., Mercer, W. E., Kinzler, K. W., and Vogelstein, B. (1993). WAF1, a potential mediator of p53 tumor suppression. *Cell*, 75(4):817–25.

Feng, L., Lin, T., Uranishi, H., Gu, W., and Xu, Y. (2005). Functional analysis of the roles of posttranslational modifications at the p53 C terminus in regulating p53 stability and activity. *Molecular and cellular biology*, 25(13):5389–95.

Fujiwara, T., Bandi, M., Nitta, M., Ivanova, E. V., Bronson, R. T., and Pellman, D. (2005). Cytokinesis failure generating tetraploids promotes tumorigenesis in p53-null cells. *Nature*, 437(7061):1043–7.

Galipeau, P. C., Cowan, D. S., Sanchez, C. A., Barrett, M. T., Emond, M. J., Levine, D. S., Rabinovitch, P. S., and Reid, B. J. (1996). 17p (p53) allelic losses, 4N (G2/tetraploid) populations, and progression to aneuploidy in Barrett's esophagus. *Proceedings of the National Academy of Sciences of the United States of America*, 93(14):7081–4.

Ganem, N. J., Godinho, S. a., and Pellman, D. (2009). A mechanism linking extra centrosomes to chromosomal instability. *Nature*, 460(7252):278–82.

Giannakakou, P., Sackett, D. L., Ward, Y., Webster, K. R., Blagosklonny, M. V., and Fojo, T.

(2000). P53 Is Associated With Cellular Microtubules and Is Transported To the Nucleus By Dynein. *Nature cell biology*, 2(10):709–17.

Gisselsson, D., Hå kanson, U., Stoller, P., Marti, D., Jin, Y., Rosengren, A. H., Stewénius, Y., Kahl, F., and Panagopoulos, I. (2008). When the genome plays dice: circumvention of the spindle assembly checkpoint and near-random chromosome segregation in multipolar cancer cell mitoses. *PloS one*, 3(4):e1871.

Gordon, D. J., Resio, B., and Pellman, D. (2012). Causes and consequences of aneuploidy in cancer. *Nature reviews. Genetics*, 13(3):189–203.

Graeber, T. G., Peterson, J. F., Tsai, M., Monica, K., Fornace, a. J., and Giaccia, a. J. (1994). Hypoxia induces accumulation of p53 protein, but activation of a G1-phase checkpoint by low-oxygen conditions is independent of p53 status. *Molecular and cellular biology*, 14(9):6264–77.

Guerrero, A. A., Gamero, M. C., Trachana, V., Fütterer, A., Pacios-Bras, C., Díaz-Concha, N. P., Cigudosa, J. C., Martínez-A, C., and van Wely, K. H. M. (2010). Centromere-localized breaks indicate the generation of DNA damage by the mitotic spindle. *Proceedings of the National Academy of Sciences of the United States of America*, 107(9):4159–64.

Guidotti, J.-E., Brégerie, O., Robert, A., Debey, P., Brechot, C., and Desdouets, C. (2003). Liver cell polyplloidization: a pivotal role for binuclear hepatocytes. *The Journal of biological chemistry*, 278(21):19095–101.

Guo, Z., Kozlov, S., Lavin, M. F., Person, M. D., and Paull, T. T. (2010). ATM activation by oxidative stress. *Science (New York, N.Y.)*, 330(6003):517–21.

Gutiérrez-Uzquiza, A., Arechederra, M., Bragado, P., Aguirre-Ghiso, J. a., and Porras, A. (2012). p38 α mediates cell survival in response to oxidative stress via induction of antioxidant genes: effect on the p70S6K pathway. *The Journal of biological chemistry*, 287(4):2632–42.

Haruki, N., Harano, T., Masuda, a., Kiyono, T., Takahashi, T., Tatematsu, Y., Shimizu, S., Mitsudomi, T., Konishi, H., Osada, H., and Fujii, Y. (2001). Persistent increase in chromosome instability in lung cancer: possible indirect involvement of p53 inactivation. *The American journal of pathology*, 159(4):1345–52.

Hasle, H., Aricò, M., Basso, G., Biondi, A., Cantù Rajnoldi, A., Creutzig, U., Fenu, S., Fonatsch, C., Haas, O. A., Harbott, J., Kardos, G., Kerndrup, G., Mann, G., Niemeyer, C. M., Ptoszkova, H., Ritter, J., Slater, R., Starý, J., Stollmann-Gibbels, B., Testi, A. M., van

- Wering, E. R., and Zimmermann, M. (1999). Myelodysplastic syndrome, juvenile myelomonocytic leukemia, and acute myeloid leukemia associated with complete or partial monosomy 7. European Working Group on MDS in Childhood (EWOG-MDS). *Leukemia*, 13(3):376–85.
- Hassold, T. and Chiu, D. (1985). Maternal age-specific rates of numerical chromosome abnormalities with special reference to trisomy. *Human genetics*, 70(1):11–7.
- Hirao, a. (2000). DNA Damage-Induced Activation of p53 by the Checkpoint Kinase Chk2. *Science*, 287(5459):1824–1827.
- Hirokawa, N. (1998). Kinesin and Dynein Superfamily Proteins and the Mechanism of Organelle Transport. *Science*, 279(5350):519–526.
- Hofseth, L. J., Saito, S., Hussain, S. P., Espey, M. G., Miranda, K. M., Araki, Y., Jhappan, C., Higashimoto, Y., He, P., Linke, S. P., Quezado, M. M., Zurer, I., Rotter, V., Wink, D. A., Appella, E., and Harris, C. C. (2003). Nitric oxide-induced cellular stress and p53 activation in chronic inflammation. *Proceedings of the National Academy of Sciences of the United States of America*, 100(1):143–8.
- Högnäs, G., Tuomi, S., Veltel, S., Mattila, E., Murumägi, a., Edgren, H., Kallioniemi, O., and Ivaska, J. (2012). Cytokinesis failure due to derailed integrin traffic induces aneuploidy and oncogenic transformation in vitro and in vivo. *Oncogene*, 31(31):3597–606.
- Janssen, A., van der Burg, M., Szuhai, K., Kops, G. J. P. L., and Medema, R. H. (2011). Chromosome segregation errors as a cause of DNA damage and structural chromosome aberrations. *Science (New York, N.Y.)*, 333(6051):1895–8.
- Jin, Y., Lee, H., Zeng, S. X., Dai, M.-s., and Lu, H. (2003). independently of ubiquitylation. 22(23):6365–6377.
- Kim, I. S., Kim, D. H., Han, S. M., Chin, M. U., Nam, H. J., Cho, H. P., Choi, S. Y., Song, B. J., Kim, E. R., Bae, Y. S., and Moon, Y. H. (2000). Truncated form of importin alpha identified in breast cancer cell inhibits nuclear import of p53. *The Journal of biological chemistry*, 275(30):23139–45.
- Kuffer, C., Kuznetsova, A. Y., and Storchová, Z. (2013). Abnormal mitosis triggers p53-dependent cell cycle arrest in human tetraploid cells. *Chromosoma*, 122(4):305–18.

- Kumari, G., Ulrich, T., and Gaubatz, S. (2013). A role for p38 in transcriptional elongation of p21 (CIP1) in response to Aurora B inhibition. *Cell cycle (Georgetown, Tex.)*, 12(13):2051–60.
- Kuznetsova, A. Y. (2013). *Transient tetraploidy as a route to chromosomal instability*. PhD thesis, Ludwig Maximillian University Munich.
- Kwon, M., Godinho, S. a., Chandhok, N. S., Ganem, N. J., Azioune, A., Thery, M., and Pellman, D. (2008). Mechanisms to suppress multipolar divisions in cancer cells with extra centrosomes. *Genes & development*, 22(16):2189–203.
- Landgraf, M., Baylies, M., and Bate, M. (1999). Muscle founder cells regulate defasciculation and targeting of motor axons in the Drosophila embryo. *Current biology : CB*, 9(11):589–92.
- Le Beau, M. M., Albain, K. S., Larson, R. A., Vardiman, J. W., Davis, E. M., Blough, R. R., Golomb, H. M., and Rowley, J. D. (1986). Clinical and cytogenetic correlations in 63 patients with therapy-related myelodysplastic syndromes and acute nonlymphocytic leukemia: further evidence for characteristic abnormalities of chromosomes no. 5 and 7. *Journal of clinical oncology : official journal of the American Society of Clinical Oncology*, 4(3):325–45.
- Lee, K., Kenny, A. E., and Rieder, C. L. (2010). P38 mitogen-activated protein kinase activity is required during mitosis for timely satisfaction of the mitotic checkpoint but not for the fidelity of chromosome segregation. *Molecular biology of the cell*, 21(13):2150–60.
- Lengauer, C., Kinzler, K. W., and Vogelstein, B. (1997). Genetic instability in colorectal cancers. *Nature*, 386(6625):623–7.
- Li, M., Fang, X., Baker, D. J., Guo, L., Gao, X., Wei, Z., Han, S., van Deursen, J. M., and Zhang, P. (2010). The ATM-p53 pathway suppresses aneuploidy-induced tumorigenesis. *Proceedings of the National Academy of Sciences of the United States of America*, 107(32):14188–93.
- Lowe, S. W. and Ruley, H. E. (1993). Stabilization of the p53 tumor suppressor is induced by adenovirus 5 E1A and accompanies apoptosis. *Genes & Development*, 7(4):535–545.
- Luna-Fineman, S., Shannon, K. M., and Lange, B. J. (1995). Childhood monosomy 7: epidemiology, biology, and mechanistic implications. *Blood*, 85(8):1985–99.
- Lv, L., Zhang, T., Yi, Q., Huang, Y., Wang, Z., Hou, H., Zhang, H., Zheng, W., Hao, Q., Guo, Z., Cooke, H. J., and Shi, Q. (2012). Tetraploid cells from cytokinesis failure induce

aneuploidy and spontaneous transformation of mouse ovarian surface epithelial cells © 2012 Landes Bioscience . Do not distribute . © 2012 Landes Bioscience . Do not distribute . 11(15):2864–2875.

Ly, P., Eskiocak, U., Kim, S. B., Roig, A. I., Hight, S. K., Lulla, D. R., Zou, Y. S., Batten, K., Wright, W. E., and Shay, J. W. (2011). Characterization of aneuploid populations with trisomy 7 and 20 derived from diploid human colonic epithelial cells. *Neoplasia (New York, N.Y.)*, 13(4):348–57.

Maki, C. G. (2010). *p53 Localization*, volume 1 of *Molecular Biology Intelligence Unit*. Springer US, Boston, MA.

Malkin, D., Li, F. P., Strong, L. C., Fraumeni, J. F., Nelson, C. E., Kim, D. H., Kassel, J., Gryka, M. a., Bischoff, F. Z., and Tainsky, M. a. (1990). Germ line p53 mutations in a familial syndrome of breast cancer, sarcomas, and other neoplasms. *Science (New York, N.Y.)*, 250(4985):1233–8.

Margall-Ducos, G., Celton-Morizur, S., Couton, D., Brégerie, O., and Desdouets, C. (2007). Liver tetraploidization is controlled by a new process of incomplete cytokinesis. *Journal of cell science*, 120(Pt 20):3633–9.

Masramon, L., Ribas, M., Cifuentes, P., Arribas, R., García, F., Egózcue, J., Peinado, M. a., and Miró, R. (2000). Cytogenetic characterization of two colon cell lines by using conventional G-banding, comparative genomic hybridization, and whole chromosome painting. *Cancer genetics and cytogenetics*, 121(1):17–21.

Matzke, M. a., Florian Mette, M., Kanno, T., and Matzke, A. J. (2003). Does the intrinsic instability of aneuploid genomes have a causal role in cancer? *Trends in Genetics*, 19(5):253–256.

Michel, L. S., Liberal, V., Chatterjee, A., Kirchwegger, R., Pasche, B., Gerald, W., Dobles, M., Sorger, P. K., Murty, V. V., and Benezra, R. (2001). MAD2 haplo-insufficiency causes premature anaphase and chromosome instability in mammalian cells. *Nature*, 409(6818):355–9.

Migeon, B. R., Norum, R. A., and Corsaro, C. M. (1974). Isolation and analysis of somatic hybrids derived from two human diploid cells. *Proceedings of the National Academy of Sciences of the United States of America*, 71(3):937–41.

Mikule, K., Delaval, B., Kaldis, P., Jurczyk, A., Hergert, P., and Doxsey, S. (2006). Loss of centrosome integrity induces p38—p53—p21-dependent G1—S arrest. *Nature Cell Biology*, 9(2):160–170.

Moll, U. M. and Petrenko, O. (2003). The MDM2-p53 interaction. *Molecular cancer research : MCR*, 1(14):1001–8.

Moll, U. T. E. M., Ostermeyer, A. G., Haladay, R., Winkfield, B., Frazier, M., and Zambetti, G. (1996). Cytoplasmic sequestration of wild-type p53 protein impairs the G1 checkpoint after DNA damage . Cytoplasmic Sequestration of Wild-Type p53 Protein Impairs the G 1 Checkpoint after DNA Damage.

Müller, C., Gross, D., Sarli, V., Gartner, M., Giannis, A., Bernhardt, G., and Buschauer, A. (2007). Inhibitors of kinesin Eg5: antiproliferative activity of monastrol analogues against human glioblastoma cells. *Cancer chemotherapy and pharmacology*, 59(2):157–64.

Mullins, J. M. and Bieseile, J. J. (1977). Terminal phase of cytokinesis in D-98s cells. *The Journal of cell biology*, 73(3):672–84.

Musacchio, A. and Salmon, E. D. (2007). The spindle-assembly checkpoint in space and time. *Nature reviews. Molecular cell biology*, 8(5):379–93.

Nigg, E. A. (2002). Centrosome aberrations: cause or consequence of cancer progression? *Nature reviews. Cancer*, 2(11):815–25.

Normand, G. and King, R. W. (2010). Understanding cytokinesis failure. *Advances in experimental medicine and biology*, 676:27–55.

Olaharski, A. J., Sotelo, R., Solorza-Luna, G., Gonsebatt, M. E., Guzman, P., Mohar, A., and Eastmond, D. a. (2006). Tetraploidy and chromosomal instability are early events during cervical carcinogenesis. *Carcinogenesis*, 27(2):337–43.

Pampalona, J., Frías, C., Genescà, A., and Tusell, L. (2012). Progressive telomere dysfunction causes cytokinesis failure and leads to the accumulation of polyploid cells. *PLoS genetics*, 8(4):e1002679.

Raingeaud, J., Gupta, S., Rogers, J. S., Dickens, M., Han, J., Ulevitch, R. J., and Davis, R. J. (1995). Pro-inflammatory cytokines and environmental stress cause p38 mitogen-activated protein kinase activation by dual phosphorylation on tyrosine and threonine. *The Journal of biological chemistry*, 270(13):7420–6.

Rivlin, N., Brosh, R., Oren, M., and Rotter, V. (2011). Mutations in the p53 Tumor Suppressor Gene: Important Milestones at the Various Steps of Tumorigenesis. *Genes \& cancer*, 2(4):466–74.

Ruiz Gómez, M. and Bate, M. (1997). Segregation of myogenic lineages in Drosophila requires numb. *Development (Cambridge, England)*, 124(23):4857–66.

Russo, G., Isobe, M., Pegoraro, L., Finan, J., Nowell, P. C., and Croce, C. M. (1988). Molecular analysis of a t(7;14)(q35;q32) chromosome translocation in a T cell leukemia of a patient with ataxia telangiectasia. *Cell*, 53(1):137–44.

Sansregret, L., Vadnais, C., Livingstone, J., Kwiatkowski, N., Awan, A., Cadieux, C., Leduy, L., Hallett, M. T., and Nepveu, A. (2011). Cut homeobox 1 causes chromosomal instability by promoting bipolar division after cytokinesis failure. *Proceedings of the National Academy of Sciences of the United States of America*, 108(5):1949–54.

Schnapp, B. J. and Reese, T. S. (1989). Dynein is the motor for retrograde axonal transport of organelles. *Proceedings of the National Academy of Sciences of the United States of America*, 86(5):1548–52.

Secchiero, P., Bertolaso, L., Casareto, L., Gibellini, D., Vitale, M., Bemis, K., Aleotti, a., Capitani, S., Franchini, G., Gallo, R. C., and Zauli, G. (1998). Human herpesvirus 7 infection induces profound cell cycle perturbations coupled to disregulation of cdc2 and cyclin B and polyploidization of CD4(+) T cells. *Blood*, 92(5):1685–96.

Shaltiel, I. a., Aprelia, M., Saurin, A. T., Chowdhury, D., Kops, G. J. P. L., Voest, E. E., and Medema, R. H. (2014). Distinct phosphatases antagonize the p53 response in different phases of the cell cycle. *Proceedings of the National Academy of Sciences of the United States of America*, 2:17–19.

Sharp, D. J. and Ross, J. L. (2012). Microtubule-severing enzymes at the cutting edge. *Journal of cell science*, 125(Pt 11):2561–9.

She, Q. B., Chen, N., and Dong, Z. (2000). ERKs and p38 kinase phosphorylate p53 protein at serine 15 in response to UV radiation. *The Journal of biological chemistry*, 275(27):20444–9.

Shi, Q. and King, R. W. (2005). Chromosome nondisjunction yields tetraploid rather than aneuploid cells in human cell lines. *Nature*, 437(7061):1038–42.

- Shieh, S. Y., Ikeda, M., Taya, Y., and Prives, C. (1997). DNA damage-induced phosphorylation of p53 alleviates inhibition by MDM2. *Cell*, 91(3):325–34.
- Shiloh, Y. (2003). ATM and related protein kinases: safeguarding genome integrity. *Nature reviews. Cancer*, 3(3):155–68.
- Storchova, Z. and Kuffer, C. (2008). The consequences of tetraploidy and aneuploidy. *Journal of cell science*, 121(Pt 23):3859–66.
- Storchova, Z. and Pellman, D. (2004). From polyploidy to aneuploidy, genome instability and cancer. *Nature reviews. Molecular cell biology*, 5(1):45–54.
- Tewey, K. M., Rowe, T. C., Yang, L., Halligan, B. D., and Liu, L. F. (1984). Adriamycin-induced DNA damage mediated by mammalian DNA topoisomerase II. *Science (New York, N.Y.)*, 226(4673):466–8.
- The Cancer Genome Atlas Research Network (2014). Comprehensive molecular characterization of urothelial bladder carcinoma. *Nature*, 507(7492):315–22.
- Thompson, S. L. and Compton, D. a. (2008). Examining the link between chromosomal instability and aneuploidy in human cells. *The Journal of cell biology*, 180(4):665–72.
- Thompson, S. L. and Compton, D. a. (2010). Proliferation of aneuploid human cells is limited by a p53-dependent mechanism. *The Journal of cell biology*, 188(3):369–81.
- Tibbetts, R. S., Brumbaugh, K. M., Williams, J. M., Sarkaria, J. N., Cliby, W. A., Shieh, S.-y., Taya, Y., Prives, C., and Abraham, R. T. (1999). A role for ATR in the DNA damage-induced phosphorylation of p53 A role for ATR in the DNA phosphorylation of p53. pages 152–157.
- Toledo, F. and Wahl, G. M. (2006). Regulating the p53 pathway: in vitro hypotheses, in vivo veritas. *Nature reviews. Cancer*, 6(12):909–23.
- Trostel, S. Y., Sackett, D. L., and Fojo, T. (2006). Oligomerization of p53 Precedes its Association with Dynein ACKNOWLEDGEMENTS ND SC INTRODUCTION. (October):2253–2259.
- Varley, J. M. (2003). Germline TP53 mutations and Li-Fraumeni syndrome. *Human mutation*, 21(3):313–20.

Vitale, I., Galluzzi, L., Senovilla, L., Criollo, a., Jemaà, M., Castedo, M., and Kroemer, G. (2011). Illicit survival of cancer cells during polyploidization and depolyploidization. *Cell death and differentiation*, 18(9):1403–13.

Vitale, I., Senovilla, L., Galluzzi, L., Criollo, A., Vivet, S., Castedo, M., and Kroemer, G. (2008). Chk1 inhibition activates p53 through p38 MAPK in tetraploid cancer cells. *Cell cycle (Georgetown, Tex.)*, 7(13):1956–61.

Vitale, I., Senovilla, L., Jemaà, M., Michaud, M., Galluzzi, L., Kepp, O., Nanty, L., Criollo, A., Rello-Varona, S., Manic, G., Métivier, D., Vivet, S., Tajeddine, N., Joza, N., Valent, A., Castedo, M., and Kroemer, G. (2010). Multipolar mitosis of tetraploid cells: inhibition by p53 and dependency on Mos. *The EMBO journal*, 29(7):1272–84.

Wang, X., Zhou, Y.-X., Qiao, W., Tominaga, Y., Ouchi, M., Ouchi, T., and Deng, C.-X. (2006). Overexpression of aurora kinase A in mouse mammary epithelium induces genetic instability preceding mammary tumor formation. *Oncogene*, 25(54):7148–58.

Warfel, N. a. and El-Deiry, W. S. (2013). p21WAF1 and tumourigenesis: 20 years after. *Current opinion in oncology*, 25(1):52–8.

Zhou, S., Palmeira, C. M., and Wallace, K. B. (2001). Doxorubicin-induced persistent oxidative stress to cardiac myocytes. *Toxicology letters*, 121(3):151–7.

9 Acknowledgments

I would like to thank Dr. Zuzana Storchova for the opportunity to perform my master thesis in her lab and for her guidance and advice regarding my thesis.

Furthermore I would like to thank Professor Dr. Stefan Jentsch for being my internal supervisor at the LMU biology department.

I'm very grateful to Dr. Anastasia Kuznetsova for her great support and supervision during my thesis.

For revisions on my thesis I would like to thank Verena Passerini.

I would like to express my gratitude to all the people from the Storchova group which made my thesis a very nice experience. Thank you for all the scientific and non-scientific talks.

I would like to thank Tobi for his love, patience and support throughout my thesis and everything beyond.

Last but not least, I would like to thank my family and Tobi's family for their support and faith in me.